
An Analysis of the Adaptation Speed of Causal Models

Rémi Le Priol¹ Reza Babanezhad Harikandeh² Yoshua Bengio^{1,3} Simon Lacoste-Julien^{1,2,3}

Abstract

We consider the problem of discovering the causal process that generated a collection of datasets. We assume that all these datasets were generated by unknown sparse interventions on a structural causal model (SCM) G , that we want to identify. Recently, Bengio et al. (2020) argued that among all SCMs, G is the *fastest to adapt* from one dataset to another, and proposed a meta-learning criterion to identify the causal direction in a two-variable SCM. While the experiments were promising, the theoretical justification was incomplete. Our contribution is a theoretical investigation of the adaptation speed of simple two-variable SCMs. We use convergence rates from stochastic optimization to justify that a relevant proxy for adaptation speed is distance in parameter space after intervention. Using this proxy, we show that the SCM with the correct causal direction is advantaged for categorical and normal cause-effect datasets when the intervention is on the cause variable. When the intervention is on the effect variable, we provide a more nuanced picture which highlights that the ‘fastest to adapt’ heuristic is not always valid. Code to reproduce experiments is available at <https://github.com/remilepriol/causal-adaptation-speed>

1. Introduction

If we elevated London by 1km, it would likely lose a few degrees. In this sense, the altitude of a city is a causal variable for its average temperature. In more general terms, a variable X is a causal variable for another variable Y if changing the value of X with some *intervention* also affects Y . On the other hand, changing the temperature of a city (e.g., with heating and transportation) would not affect its altitude. This asymmetric relationship contains important

information besides the joint distribution between the two variables, information which is important for learning agents because it is crucial for deciding how to act, in order to obtain desired effects. This definition of causal relationship can be generalized to many variables with the formalism of *structural causal models* (SCM) (Pearl, 2009; Peters et al., 2017). SCMs are a kind of Bayesian Network, a generative models which decompose the generative process of the data as a succession of mechanisms and add a causal attribute to the edges of the graphical model, now called a causal graph. A key assumption is that SCM’s arrows are indicative of time and of an asymmetric cause-effect relationship: in case of interventions on X , only variables downstream of X are (later) affected.

Another key assumption which is associated with causal modeling is the *Independent Mechanism Principle* (Janzing & Scholkopf, 2010): knowing something about one causal mechanism (e.g. how Y is affected by a direct cause X) does not inform us about other mechanisms (e.g. how X was generated in the first place). This principle has an important consequence for machine learning, especially if we want to expand current methods to make them more robust to changes in data distribution or to non-stationarities in the environment, a problem referred to as *external validity* in statistics (Pearl & Bareinboim, 2014). Whereas the classical theoretical analysis of learning algorithms relies on the assumption that the test cases will come from the same distribution as the training examples, this is not a realistic assumption in practice, causing practical issues when deploying machine learning systems. How can we build learning machines which behave robustly out-of-distribution? If they are allowed to adapt, as in transfer learning, how do we make sure the sample complexity for adapting to the modified distribution is small? One issue, when considering these questions is that if we get rid of the iid assumption which is the basis of traditional learning theory for generalizing to test cases (from the same distribution as the training examples), we need to replace it with other assumptions, or we will not be able to say anything about future cases. The Independent Mechanism Principle, along with modeling of causal dependencies, can be a good start, as we argue here in a very simple scenario.

To see this more concretely, assume a learning agent is faced with a distribution shift due to one mechanism change

¹Mila, Université de Montreal ²SAIT AI Lab, Montreal
³Canada CIFAR AI Chair. Correspondence to: Remi Le Priol
<lepriol@mila.quebec>.

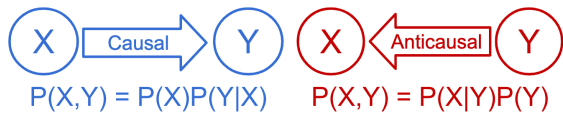


Figure 1. Two parametrizations of cause-effect data $X \rightarrow Y$.

(typically due to an intervention by some agent, initially affecting only one causal variable). If the learning agent observing data from the old and the new distribution knows the correct causal model, then it will have to adapt only one of its mechanisms (the one which was the subject of the intervention) to account for the change in distribution. From this idea, [Bengio et al. \(2020\)](#) recently proposed that such an agent will *adapt faster* to the modified distribution than an agent with an incorrect causal model. Their main argument is that with the correct causal model, fewer mechanisms and thus fewer parameters need to be adapted to account for the change in distribution. They verify this claim empirically for a simple two variables cause-effect SCM $X \rightarrow Y$ (Figure 1), and they derive a meta-learning criterion to identify the arrow direction. [Ke et al. \(2019\)](#) generalize this approach to multiple variables and causal dependencies described by an arbitrary causal graph.

Although less mechanisms to adapt does usually mean less parameters to update, what has been lacking is a theoretical demonstration of how and when this may translate into fast adaptation. The heuristic argument from [Bengio et al. \(2020\)](#) is that one needs more samples to estimate more parameters. This is justified by the remark that a smaller effective model capacity, e.g. smaller VC-dimension ([Vapnik & Chervonenkis, 1971](#)), turns into a smaller generalization gap ([Ehrenfeucht et al., 1989](#)). This reasoning is appealing but not perfectly coherent with their setting, which motivates the theoretical analysis in our paper. In particular, they use stochastic gradient descent to estimate new parameters. This algorithm has sample complexity bounds which typically do not depend on the number of parameters to update ([Bubeck et al., 2015](#), Th. 6.2 & 6.3), which seems to contradict the above argument. In this work, we close this gap by providing an analysis of the relationship between interventions and adaptation speed directly using stochastic gradient descent convergence results.

Contributions. We investigate the adaptation speed of two-variable SCMs in two settings: a categorical and a normal cause-effect model. We showcase convergence rates of stochastic optimization algorithms that apply to these settings and provide simple sample complexity bounds. These bounds mainly depend on the distance in parameter space between the initialization (before intervention) and the optimum (which is the parameter of the distribution after intervention), which we use as a proxy to analyze the adaptation

speed. When the intervention is on the cause variable, we prove that the causal model has a smaller distance to cross than the anticausal model, which supports the claim that the causal model is faster to adapt. We corroborate this claim with empirical observations that the adaptation speed is well correlated with the initial distance, and that the causal model is faster than the anticausal model. When the intervention is on the effect, we provide a more nuanced picture which depends on how the parameters are chosen, highlighting that the causal model is not necessarily advantaged.

2. Related Work

Causal relationships are asymmetric. These asymmetries are often visible in observations, so that one can identify which is cause and which is effect under relevant assumptions ([Mooij et al., 2016](#)). A common assumption is to constrain the set of functional dependencies between cause and effect. By contrast, in our work, we focus on two families of distributions which are notoriously unidentifiable from observational data: categorical and linear normal variables ([Peters et al., 2017](#), Ch.4). To discover the direction, we need access to interventional data.

Inferring causal links from interventions or experiments is the foundation of science. Inferring causal links from unknown interventions is a much harder and less principled problem. Among the large body of work produced on this topic, [Tian & Pearl \(2001\)](#) is perhaps the closest to ours. They observe a sequence of distributions, where each distribution differ from the previous one by a single unknown mechanism change. They propose a statistical method that infer a causal structure. From a machine learning perspective, we are concerned with the predictive power that this structure will give us when faced with new data.

Since the work of [Schölkopf et al. \(2012\)](#), the idea of *invariance* has emerged in the machine learning literature as a principle to tackle distribution shifts. If some law or correlation is invariant across several different datasets, then it might be causal, and it is likely to hold true in the future. Based on this idea, [Peters et al. \(2016\)](#) designed an algorithm able to identify robust causal features from heterogeneous data. This work has set a fruitful line of research for robust machine learning ([Heinze-Deml et al., 2018b;a](#); [Rothenhäusler et al., 2019](#); [Arjovsky et al., 2019](#)). In a way, fast adaptation is the complementary idea of invariance: if most mechanisms are kept invariant, then only a few have to adapt. [Schölkopf \(2019\)](#) shed light on these approaches and the broader scope of causality research for machine learning.

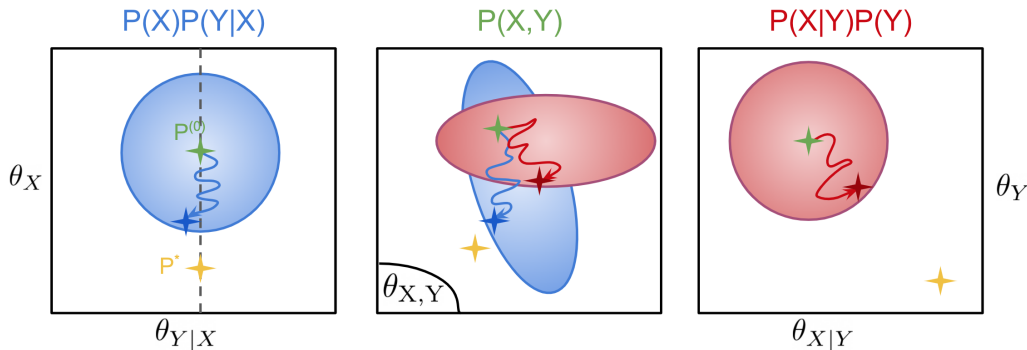


Figure 2. An intuitive sketch showing how the causal model can be faster to adapt to an unknown intervention. *Left*: causal parameter space. *Right*: anticausal parameter space. *Middle*: joint model abstract representation where the distance is somewhat representative of the KL. *Green Star*: reference distribution $\mathbf{p}^{(0)}$. *Golden Star*: target distribution \mathbf{p}^* coming from an intervention on the cause (change in θ_X only in the left panel). *Blue Path*: update path taken by SGD in the causal model. It reaches the *Blue Star* after seeing a few samples. We map this path from the causal parameter space to the joint space. *Red Path and Circle*: same for anticausal model. **Interpretation**: The causal model only has to adapt its marginal mechanism θ_X , whereas the anticausal model has to adapt both mechanisms. It has to cross a larger region in parameter space. The blue and red balls represent the *proximity prior* enforced by taking a few steps of SGD from the reference distribution in each parameter space. Convergence rate analysis reveals that they are approximately spherical in their parameter space – e.g. they are proportional to the distance – but they are mapped to non-trivial shapes in distribution space – ellipses in this sketch.

3. Background

In this section, we review the formalism of Bengio et al. (2020) on observations, interventions, models and adaptation.

Reference and Transfer Distributions. We assume infinite access to a reference distribution \mathbf{p} over the joint variable X, Y . This distribution is the object of interventions, which results in new *transfer* distributions \mathbf{p}^* . If the *intervention is on the cause*, X is sampled from a different marginal, then Y is sampled from the reference conditional

$$\mathbf{p}^*(x, y) = \mathbf{p}(y|x)\mathbf{p}^*(x).$$

If the *intervention is on the effect*, X is sampled from the reference marginal, then Y is sampled from another marginal independently of X

$$\mathbf{p}^*(x, y) = \mathbf{p}(x)\mathbf{p}^*(y).$$

For each transfer distribution, we observe a few samples.

Models. We parametrize two generative models of (X, Y) (Figure 1):

$$\mathbf{p}_{\theta_{\rightarrow}}(x, y) = \mathbf{p}_{\theta_X}(x)\mathbf{p}_{\theta_{Y|X}}(y|x) \quad - \text{causal} \quad (1)$$

$$\mathbf{p}_{\theta_{\leftarrow}}(x, y) = \mathbf{p}_{\theta_Y}(y)\mathbf{p}_{\theta_{X|Y}}(x|y) \quad - \text{anticausal} \quad (2)$$

For each model, we call mechanisms the marginal and conditional models. Each mechanism has its own set of parameters, e.g. θ_X and $\theta_{Y|X}$. In the following we will use θ to denote interchangeably θ_{\rightarrow} and θ_{\leftarrow} .

Adaptation. Both models are initialized to fit perfectly the reference distribution $\mathbf{p}_{\theta_{\rightarrow}^{(0)}} = \mathbf{p}_{\theta_{\leftarrow}^{(0)}} = \mathbf{p}$. They observe fresh samples from \mathbf{p}^* one by one and update their parameters θ_{\rightarrow} and θ_{\leftarrow} to maximize the log-likelihood with a step of stochastic gradient. Thanks to the separate parameters, the causal model log-likelihood loss decomposes as

$$\begin{aligned} \mathcal{L}_{\text{causal}}(\theta_{\rightarrow}) &= \mathbb{E}_{(X,Y) \sim \mathbf{p}^*} [-\log \mathbf{p}_{\theta_{\rightarrow}}(X, Y)] \\ &= \mathbb{E}_{\mathbf{p}^*} [-\log \mathbf{p}_{\theta_X}(X)] + \mathbb{E}_{\mathbf{p}^*} [-\log \mathbf{p}_{\theta_{Y|X}}(Y|X)] \end{aligned} \quad (3)$$

When \mathbf{p}^* comes from an intervention, Bengio et al. (2020) observe that the causal model is often faster to adapt than the anticausal model. Intuitively, this is because the causal model has to adapt only the mechanism which was modified by the intervention. On the other hand, the anticausal model has to adapt both its mechanisms. In Figure 2, we compare these different scenarios and the concept of adaptation figuratively. In the next section, we present an approach based on the convergence speed of stochastic optimization methods to formalize and understand this phenomenon.

Distribution Families. We explore two simple families: categorical and linear normal variables. These families are interesting because the direction is not identifiable from observational data (Peters et al., 2017, Ch.4) – e.g. $\mathbf{p}_{\theta_{\rightarrow}}$ and $\mathbf{p}_{\theta_{\leftarrow}}$ can model the same set of distributions – which makes them challenging for causal discovery.

4. An Optimization Perspective

One way to formalize adaptation speed is to characterize it via the convergence speed of the stochastic optimization

procedure. An appealing aspect of stochastic optimization algorithms such as SGD (when only using fresh samples and running it on the true loss we care about) is that they come with convergence rate guarantees on the *population risk* in machine learning, thus giving us direct sample complexity results to obtain a specific generalization error. The convergence rate is an *upper bound* on the expected suboptimality after a given number of iterations. While these rates are about worst case performance and might also be loose, fortunately, for convex optimization, they tend to correspond well to actual empirical performance (Nesterov, 2004). We can thus use the convergence bounds as theoretical proxy for the convergence speed. In our experiments, we also verify empirically that the bounds correlate well with the observed convergence speed.

Here we provide a classical convergence rate of Average Stochastic Gradient Descent (ASGD) under convexity and bounded gradient assumptions. We derive this rate in Appendix A.1 for completeness. This rate applies to the log-likelihood objective of categorical random variables (details in Appendix A.2). It takes the form of an upper bounds on the expected KL-divergence, because this is equal to the suboptimality of the log-likelihood, when the target distribution is part of the model family – e.g. $\mathcal{L}(\theta) - \mathcal{L}(\theta^*) = D_{\text{KL}}(\mathbf{p}^* || \mathbf{p}_\theta)$.

ASGD. Assume $\forall \theta, x, \|\nabla \log \mathbf{p}_\theta(x)\| \leq B$. After T iterations of SGD on (3),

$$\theta^{(t+1)} = \theta^{(t)} + \gamma \nabla \log \mathbf{p}_{\theta^{(t)}}(X_t, Y_t)$$

with learning rate $\gamma := \frac{c}{\sqrt{T}}$, starting from $\theta^{(0)}$, the average parameter $\bar{\theta}^{(T)} = \frac{1}{T} \sum_{t=0}^{T-1} \theta^{(t)}$ verifies

$$\mathbb{E} [D_{\text{KL}}(\mathbf{p}^* || \mathbf{p}_{\bar{\theta}^{(T)}})] \leq \frac{c^{-1} \|\theta^{(0)} - \theta^*\|^2 + cB^2}{2\sqrt{T}} \quad (4)$$

where the expectation is taken over the sampling of $T - 1$ training points X_t, Y_t and θ^* is the closest solution to $\theta^{(0)}$ in the solution set $\text{argmin}_\theta \mathcal{L}(\theta)$.

For categorical models, B is in between 1 and 2 (details in Appendix A.3). Consequently, for a fixed T and with small enough c , the convergence upper bounds for causal and anticausal models differ mainly by $\delta := \|\theta^{(0)} - \theta^*\|^2$.

The assumptions of this convergence rate do not apply to the optimization of normal variables. In Section 6.2, we provide an algorithm with convergence rate (12) that do apply. However both bounds (12) and (4) carry the same message which can be summarized by:

The adaptation speed is dominated by the initial distance

$$\delta_{\text{causal}} = \left\| \theta_{\rightarrow}^{(0)} - \theta_{\rightarrow}^* \right\|^2, \quad \delta_{\text{anticausal}} = \left\| \theta_{\leftarrow}^{(0)} - \theta_{\leftarrow}^* \right\|^2.$$

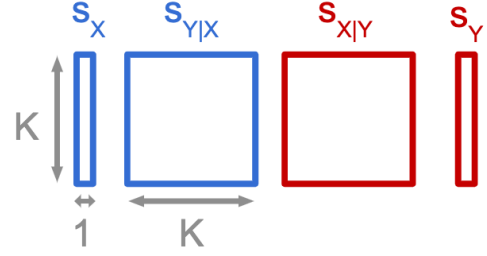


Figure 3. Parametrization of categorical models

5. Categorical Variables

In this section, both cause and effect come from categorical distribution. We show theoretically when interventions in the causal model should be advantageous. We consider different scenarios to generate reference and transfer data and explain the consequences of each scenario.

5.1. Definitions

Cause X and effect Y are now two categorical variables taking values in $\{1, \dots, K\}$. Categorical variables are an exponential family with mean parameters $\mathbf{p} \in \Delta_K$ the probability vector, and with natural parameter $\mathbf{s} \in \mathbb{R}^K$ – the logits or score parameters such that

$$p_z = \frac{e^{s_z}}{\sum_{z'} e^{s_{z'}}} \quad (5)$$

The causal model has parameters $\mathbf{s}_X := (s_x)_{x=1\dots K}$ and $\mathbf{s}_{Y|X} := (s_{y|x})_{x,y=1\dots K}$.

We gather the causal parameters in the variable $\theta_{\rightarrow} = (\mathbf{s}_X, \mathbf{s}_{Y|X})$ and the anticausal parameters in $\theta_{\leftarrow} = (\mathbf{s}_Y, \mathbf{s}_{X|Y})$. We summarize these two parametrizations in Figure 3. The generic optimization problem that we are facing is

$$\begin{aligned} f(\theta) &= \mathbb{E}_{\mathbf{p}^*} [-\log \mathbf{p}_{\theta_{\rightarrow}}(x, y)] \\ &= \mathbb{E}_{\mathbf{p}^*} [-s_x - s_{y|x}] + \log \left(\sum_{x', y'} e^{s_{x'} + s_{y'|x'}} \right). \end{aligned}$$

It is the sum of a stochastic linear loss and a deterministic softmax term. To be self-contained, in Appendix A.2 we show the well known properties of $f(\theta)$ which allow us to use the rate (4).

5.2. Distances after Interventions

In this section, we discuss formally that what happens in terms of parameter adaptation when an intervention occurs.

Intervention on cause X , $\mathbf{s}_X \leftarrow \mathbf{s}_X^*$. the causal conditional $\mathbf{s}_{Y|X}$ is left unchanged, but the effect marginal \mathbf{s}_Y

is modified in a non-trivial way. Consequently the initial distances are

$$\begin{aligned}\delta_{\text{causal}} &= \|\mathbf{s}_X - \mathbf{s}_X^*\|^2 \\ \delta_{\text{anticausal}} &= \|\mathbf{s}_Y - \mathbf{s}_Y^*\|^2 + \sum_y \|\mathbf{s}_{X|y} - \mathbf{s}_{X|y}^*\|^2.\end{aligned}$$

The causal model has to update K parameters, whereas the anticausal model has to adapt $K^2 + K$ parameters. Therefore the causal model seems to be advantaged by a factor K . The following proposition shows that this is reflected in terms of ℓ^2 distance.

Proposition 1. *When the intervention happens on the cause,*

$$\delta_{\text{anticausal}} \geq K \delta_{\text{causal}}.$$

The proof is presented in Appendix B.

Intervention on effect Y , $\forall x, \mathbf{s}_{Y|x} \leftarrow \mathbf{s}_Y^*$. Cause and effect become independent. As a result, $\forall y, \mathbf{s}_{X|y}^* = \mathbf{s}_X$. Only the marginal parameters \mathbf{s}_X is left unchanged between reference and transfer distribution. The causal model has to update the K^2 parameters in $\mathbf{s}_{Y|X}$ whereas the anticausal model has to update all of its $K^2 + K$ parameters. In other words, the causal model has to update slightly less parameters than the anticausal model. This advantage is too tiny to guarantee faster optimization. In fact, in terms of ℓ^2 distance, the causal model is advantaged only if the intervention \mathbf{s}_Y^* is close enough from the previous marginal, as formalized by the following proposition

Proposition 2. *When the intervention happens on the effect*

$$\begin{aligned}\Delta &:= \delta_{\text{causal}} - \delta_{\text{anticausal}} \\ &= (K - 1) \left(\|\mathbf{s}_Y^* - \mathbf{c}\|^2 - R^2 \right)\end{aligned}$$

where $R^2 \approx K \widehat{\text{Var}}_X[\log \sum_y e^{\mathbf{s}_{y|x}}]$, $\mathbf{c} = \frac{(\sum_x \mathbf{s}_{Y|x}) - \mathbf{s}_Y}{K-1}$.

See Appendix B.3 for the exact formula of R and the proof. To put this proposition in words, if \mathbf{s}_Y^* is within a ball of radius R centered at \mathbf{c} , then the causal model is advantaged, otherwise the anticausal model is advantaged. The intuition behind this latter behavior is that the causal model needs to move a lot the K^2 parameters of $\mathbf{s}_{Y|X}$, whereas the anticausal model needs to slightly nudge $\mathbf{s}_{X|Y}$ (size K^2) and to significantly shift \mathbf{s}_Y (size K). For "strong" interventions, the causal model has more work to do.

5.3. How to simulate $\theta^{(0)}$

To evaluate the fast adaptation criterion, we are going to work on synthetic data, which raises the question : from which distribution should we sample $\mathbf{p} = \mathbf{p}_{\theta^{(0)}}$? We call this distribution *prior*. Following the independent mechanism assumption, the marginal on the cause \mathbf{p}_X and the conditional of effect given cause $\mathbf{p}_{Y|X}$ should not contain any information about each other.

Dense Prior. To sample causal mechanisms, a natural choice is to use the uniform law over the simplex

$$\mathbf{p}_X \sim \text{Dir}(\mathbf{1}_K) \quad \text{and} \quad \forall x, \mathbf{p}_{Y|x} \sim \text{Dir}(\mathbf{1}_K) \quad (6)$$

where $\mathbf{1}_K$ is the all-one vector of dimension K . In (6), we first sample a distribution from a uniform Dirichlet to generate the law of X . Then for each value of $X = x$, we sample a uniform Dirichlet to generate the law for the conditional $Y|X = x$. We call this choice the *dense prior* by opposition to the sparse prior introduced next. This is the choice made in Bengio et al. (2020), as well as Chalupka et al. (2016). The latter work reports that distributions sampled with from this prior exhibit some asymmetry between X and Y . In Appendix C.1, we complement their work, explaining how the effect marginal is likely to be closer from the uniform distribution than the cause marginal. This asymmetry means that *the causal direction is identifiable from observational data*.

Sparse Prior. To fix this issue, we propose an alternative prior that is symmetric and ensures that both cause and effect marginals are sampled from a uniform prior over Δ_K . We sample the causal mechanisms as follows

$$\begin{aligned}\mathbf{p}_X &\sim \text{Dir}(\mathbf{1}_K) \\ \forall x, \mathbf{p}_{Y|x} &\sim \text{Dir}(\mathbf{1}_K / K).\end{aligned} \quad (7)$$

The $\mathbf{1}_K / K$ parameter means that samples will be approximately sparse, hence the name. We show in Appendix C.2 that with this sampling scheme, the joint is sampled from a sparse Dirichlet over Δ_{K^2} : $\mathbf{p}_{(X,Y)} \sim \text{Dir}(\mathbf{1}_{K^2} / K)$. This in turns means that we can switch the roles of X and Y in (7). In particular, the effect marginal has uniform density over the simplex. In general, *the causal direction is not identifiable from observational data*.

5.4. Experiments

As discussed in Section 5.3, sampling the joint distribution on X, Y from a dense or a sparse prior is going to influence the behavior of ASGD. We are asking two questions:

1. Is the adaptation speed positively correlated with the initial distance, as suggested by the upper bound (4) on the convergence rate of ASGD?
2. Under which conditions is the causal model faster to adapt?

5.4.1. EXPERIMENTAL SETUP

Data. We consider categorical variables with $K = 20$. For each initialization method, we sample 100 different reference joint distributions. For each of these distributions, *we sample an intervention by sampling a probability vector*

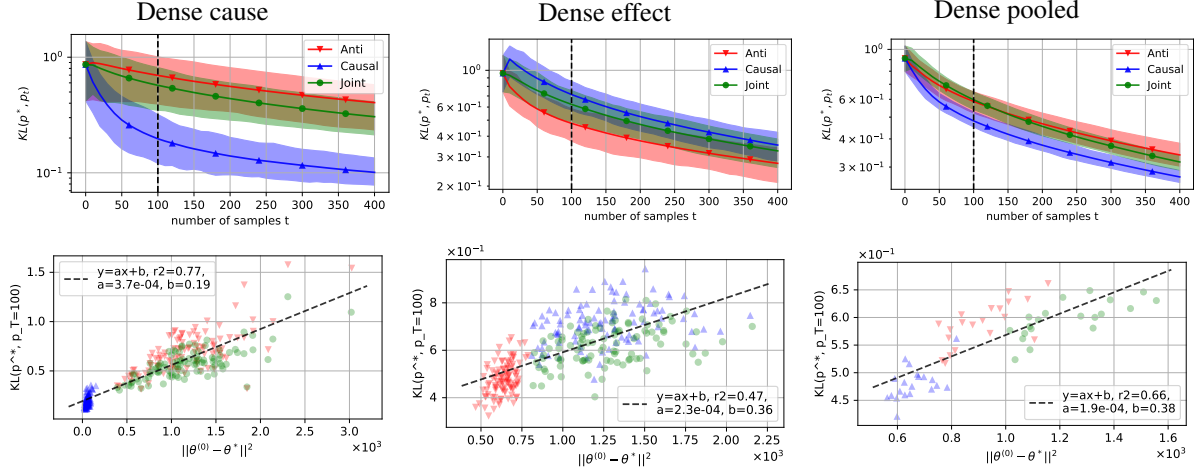


Figure 4. **Categorical dense prior with $K=20$.** Row 1: training curves. Solid lines are average KL over 100 runs. We tune hyperparameters to minimize the average KL of each model at the black vertical dashed bar ($t=100$). Shaded areas are between (5,95) quantiles. Note that *all models start from the same initial KL, but they converge at different speeds*. Row 2: scatter plot of the KL at $t=100$ vs. initial distance. Note that the initial distance is well correlated with the KL after 100 steps of SGD. Columns: we report results for interventions on the cause on column 1, the effect on column 2, and an aggregation of both on column 3. We aggregate results by taking the average of 5 cause interventions and 5 effect interventions as one new trajectory. In total we have 20 such trajectories per model. We are reporting this result because the meta-learning criterion suggested by Bengio et al. (2020) is akin to the average adaptation speed over a small set of interventions.

q uniformly from Δ_K . If the intervention is on the cause, we plug q instead of p_X . If the intervention is on the effect, we redefine $p_{Y|x} = q, \forall x$.

Models. We are comparing causal and anticausal models adaptation speed. We also report results for a model of the joint $p_{X,Y} = \text{softargmax}(s_{X,Y})$ as a reference model. We expect its results to be in between the performance of the causal and anticausal model as it expresses no prior over the direction. We optimize all models with Averaged SGD. In each iteration of SGD we get one fresh sample from the transfer distribution. For each model and each setting, we tune the learning rate so as to optimize the likelihood after seeing $\frac{K^2}{4}$ samples, to explore the few samples regime. We use a constant learning rate.

5.4.2. DENSE PRIOR

We report results with the dense prior in Figure 4. When the intervention is on the cause, the causal model is much closer from its optimum: the blue cluster is on the left of the scatter plots. This is well correlated with faster adaptation. On contrary *when the intervention is on the effect, the anticausal model is closer from its optimum* and it converges faster. We can interpret this result in light of Proposition 2. In Appendix B.3, we explain why the radius R is small under the dense prior. As a result, s_Y^* is mostly sampled outside of the ball where the causal model is advantaged. Overall the advantage of the anticausal model is weaker than the advantage of the causal model, so that if we take a balanced

average of a few interventions on the cause and a few interventions on the effect, the causal model is systematically advantaged.

5.4.3. SPARSE PRIOR

Results are in Figure 5. When the intervention is on the cause, the causal model has a small advantage. When the intervention is on the effect, no model has a set advantage, but the KL values are much higher. This is because we are taking the KL between a cross-product of marginals drawn uniformly from the simplex, and a joint drawn from the borders of the simplex (more details in C.3). The consequence of this KL explosion is that the effect intervention dominates the average KL (right panels of Figure 5), and that we cannot guess the direction from averaged adaptation curves. This practical challenge opens the door to other suggestions such as inferring the intervention, as explored by Ke et al. (2019).

6. Normal Variables

In this section, we analyze the case of two multivariate normal variables with a linear relationship. Cause X and effect Y are sampled from the causal model

$$\begin{aligned} X &\sim \mathcal{N}(\mu_X, \Sigma_X) \\ Y|X &\sim \mathcal{N}(AX + a, \Sigma_{Y|X}) \end{aligned} \quad (8)$$

with parameters $\mu_X, a \in \mathbb{R}^K$ and $\Sigma_X, A, \Sigma_{Y|X} \in \mathbb{R}^{K \times K}$. This parametrization is the most intuitive but it is unfor-

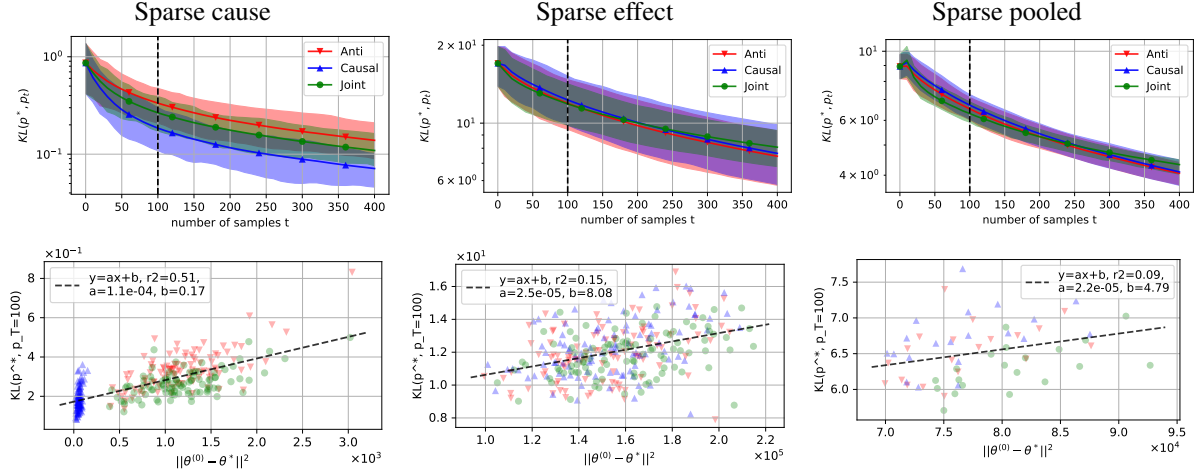


Figure 5. **Categorical sparse prior with $K=20$.** *Column 1:* intervention on the cause. The causal model starts closer from optimum and adapts slightly faster than others. *Column 2:* intervention on the effect. All models have the same initial distance and the same objective value. However the KL value is around 10. This is 10 times larger than when the intervention is on the cause. *Column 3:* we take the average of 5 effect and 5 cause interventions. The effect dominates this average because it is much larger. As a result there is no signal.

tunately not appropriate to get convergence rates. We are going to introduce another parametrization (Sec. 6.1), along with an algorithm and a convergence rate (Sec. 6.2), before providing empirical results (Sec. 6.3).

6.1. Cholesky Parametrization

The negative log-likelihood of model (8) is notoriously non-convex. This is problematic for convergence results. For simplicity, we focus in this section on the simple marginal mechanism with parameters μ, Σ . We will cover the full model in Appendix E. If we instead use the natural parameters $\eta = \Sigma^{-1}\mu$ and $\Lambda = \Sigma^{-1}$ (precision matrix), the objective is convex

$$\mathbb{E} [-\log \mathbf{p}_{(\eta, \Lambda)}(X)] = \frac{1}{2} \left(\mathbb{E} [\text{Tr}(X X^\top \Lambda) - 2X^\top \eta] + \eta^\top \Lambda^{-1} \eta - \log |\Lambda| \right). \quad (9)$$

This objective is composed of a pleasant stochastic quadratic term, and a difficult deterministic barrier objective which goes to infinity when $\Lambda \rightarrow 0$. This barrier is composed of a matrix inverse and a log determinant. The assumptions of Lipschitz or gradient-Lipschitz required to get SGD convergence do not hold for the barrier. While the empirical version of (9) has a close formed formula for its global minimum, quite surprisingly, gradient-based optimization of the normal likelihood is difficult to analyze. Convex optimization typically deals with non-smooth terms by introducing proximal operators (Parikh et al., 2014). However this barrier term is too complex to get an analytic formula for the proximal operator. Let us simplify it by introducing \mathbf{L} , the lower triangular Cholesky factor of the precision matrix $\Lambda = \mathbf{L}\mathbf{L}^\top$, and $\zeta = \mathbf{L}^{-1}\eta = \mathbf{L}^\top\mu$. Then (9) simplifies

into

$$\mathbb{E} [-\log \mathbf{p}_{(\zeta, \mathbf{L})}(X)] = \frac{1}{2} \mathbb{E} [\|\mathbf{L}^\top X - \zeta\|^2] - \sum_i \log \mathbf{L}_{i,i}. \quad (10)$$

We will refer to ζ, \mathbf{L} as *Cholesky parameters*. This objective is more suitable to gradient based optimization with a simple proximal operator, as detailed in the next section. We provide all details about the causal model in Appendix E.

6.2. Stochastic Proximal Gradient Algorithm

We want to minimize the sum of a stochastic convex smooth function $f_X(\theta) := \frac{1}{2} \|\mathbf{L}^\top X - \zeta\|^2$ and convex non-smooth regularizer $g(\theta) = -\sum_i \log \mathbf{L}_{i,i}$. This is exactly the goal of the stochastic proximal gradient (Duchi et al., 2010) update

$$\theta_{t+1} = \underset{\theta}{\text{argmin}} g(\theta) + \frac{1}{2\gamma_t} \|\theta_t - \gamma_t \nabla f_{X_t}(\theta_t) - \theta\|^2 \quad (11)$$

where γ_t is the step-size and X_t is randomly sampled. For objective (10), the proximal gradient update has a closed form solution that amounts to updating all parameters with the stochastic gradient of the quadratic term, then updating the diagonal elements of \mathbf{L} with the mapping $x \mapsto \frac{1}{2}(x + \sqrt{x^2 + 4\gamma})$ to ensure that they remain strictly positive (details in Appendix D.2).

Convergence Rate We assume that stochastic gradients ∇f_X are almost-surely B -Lipschitz. B is known as the smoothness constant. We show in Appendix D.1 that running the stochastic proximal gradient algorithm with step

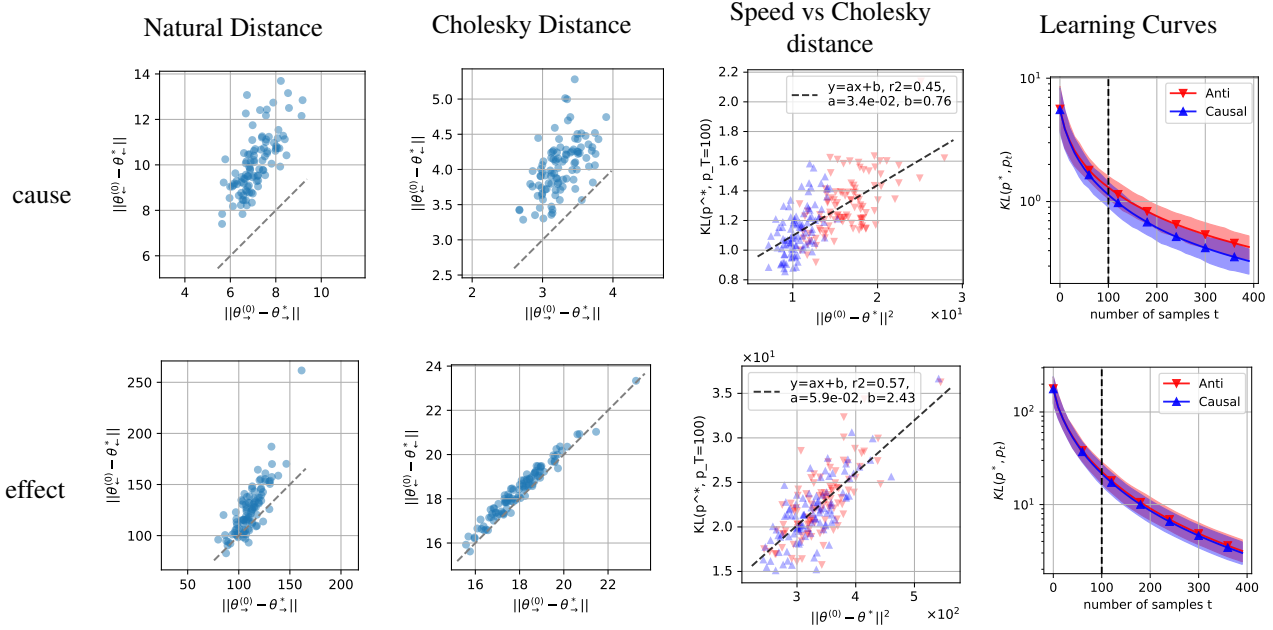


Figure 6. **Multivariate Normal Variables with dimension $K = 10$.** Row 1 and 2 correspond to interventions on cause and effect respectively. *Column 1 & 2:* scatter plot $\delta_{\text{anticausal}}$ vs δ_{causal} respectively in natural and Cholesky parametrization. The grey diagonal is the identity line. We observe a natural tendency for $\delta_{\text{anticausal}} > \delta_{\text{causal}}$ (points above the grey diagonal), but this is systematically true only for the natural distance when the intervention is on the cause. *Column 3 & 4:* same plot as in Figure 4. Once again we observe a correlation between initial distance and optimization speed. When the intervention is on the cause, the causal model is advantaged. When the intervention is on the effect, both curves overlap.

size $\gamma_t = \frac{\gamma}{\sqrt{T}} \leq \frac{1}{3B\sqrt{T}}$, for T iterations guarantees

$$\mathbb{E}[D_{\text{KL}}(\mathbf{p}^* || \mathbf{p}_{\bar{\theta}(\tau)})] \leq \frac{\|\theta^{(0)} - \theta^*\|^2}{\gamma\sqrt{T}} + \frac{D_{\text{KL}}(\mathbf{p}^* || \mathbf{p}_{\theta^{(0)}})}{T}. \quad (12)$$

Analysis. The term $\frac{D_{\text{KL}}(\mathbf{p}^* || \mathbf{p}_{\theta^{(0)}})}{T}$ is equal for causal and anticausal models because we assume $\mathbf{p}_{\theta_{\rightarrow}}^{(0)} = \mathbf{p}_{\theta_{\leftarrow}}^{(0)}$. For normal variables, B depends only on the data and is a priori equal for both models (Appendix D.3). Similarly to (4), both models' rates differ mainly by $\delta = \|\theta^{(0)} - \theta^*\|^2$.

When the intervention is on the cause, we prove in Appendix E.5 that the anticausal model is farther away from its optimum in the natural parametrization

$$\delta_{\text{anticausal}} \geq \delta_{\text{causal}}. \quad (13)$$

Unfortunately, we observe empirically that there is no such guarantee in the Cholesky parametrization, or when the intervention is on the effect.

6.3. Experiments

Similarly to categorical variables, we have to decide on how to sample reference and transfer distributions. This choice is informed by two criteria. First the independent

mechanism principle which states that we should sample θ_X independently of $\theta_{Y|X}$. Second we want θ_Y to have approximately the same distribution as θ_X – e.g. we want the distribution to be approximately symmetric so that we cannot identify the direction from observational data. These considerations lead us to the sampling scheme described in Appendix F.

We sample 100 random joint distributions from this prior, and for each distribution we sample a random intervention on the cause, and a random intervention on the effect. We then run the stochastic proximal gradient on objective (10). We report results in Figure 6. Similarly to the categorical case, when the intervention is on the cause, the causal model is advantaged by a slight margin. When the intervention is on the effect both models are learning at the same speed.

Conclusion

We provided a first theoretical analysis of the adaptation speed in two-variable cause-effect SCMs under localized interventions for categorical and normal data. Convergence guarantees for stochastic optimization on the true population log-likelihood indicate that the adaptation speed is related to the distance between initial point and optimum in parameter space. We verified this correlation empirically. We proved analytically that this distance is lower for the causal model

than for the anticausal model when the intervention is on the cause variable. This explains a surprising phenomenon: while both models start with the same suboptimality, one learns faster than the other. When the intervention is on the effect variable, we highlighted examples showing that either model can be advantaged. This provides theoretical justification for the approach of Bengio et al. (2020), while at the same time raising new questions to address, such as: which conditions could we impose on the distribution to guarantee that the causal model is still advantaged when intervening on an effect? Can we get bounds for more general distribution families than the ones considered in this paper?

ACKNOWLEDGMENTS

We thank Sébastien Lachapelle and Tristan Deleu for insightful discussions and useful feedback that led to the main results of this paper. We thank Waïss Azizian for his help in debugging the proof of Lemma B.5. This work was partially supported by the Canada CIFAR AI Chair Program. Simon Lacoste-Julien is a CIFAR Associate Fellow and Yoshua Bengio is a Program Co-Director in the Learning in Machines & Brains program.

References

- Arjovsky, M., Bottou, L., Gulrajani, I., and Lopez-Paz, D. Invariant risk minimization. *arXiv preprint arXiv:1907.02893*, 2019.
- Atchadé, Y. F., Fort, G., and Moulines, E. On perturbed proximal gradient algorithms. *Journal of Machine Learning Research*, 18(1):310–342, 2017.
- Bengio, Y., Deleu, T., Rahaman, N., Ke, R., Lachapelle, S., Bilaniuk, O., Goyal, A., and Pal, C. A meta-transfer objective for learning to disentangle causal mechanisms. In *ICLR*, 2020.
- Bubeck, S. et al. Convex optimization: Algorithms and complexity. *Foundations and Trends® in Machine Learning*, 2015.
- Chalupka, K., Eberhardt, F., and Perona, P. Estimating causal direction and confounding of two discrete variables. *arXiv preprint arXiv:1611.01504*, 2016.
- Duchi, J. and Singer, Y. Efficient online and batch learning using forward backward splitting. *Journal of Machine Learning Research*, 10(Dec):2899–2934, 2009.
- Duchi, J. C., Shalev-Shwartz, S., Singer, Y., and Tewari, A. Composite objective mirror descent. In *COLT*, pp. 14–26, 2010.
- Ehrenfeucht, A., Haussler, D., Kearns, M., and Valiant, L. A general lower bound on the number of examples needed for learning. *Information and Computation*, 1989.
- Heinze-Deml, C., Maathuis, M. H., and Meinshausen, N. Causal structure learning. *Annual Review of Statistics and Its Application*, 2018a.
- Heinze-Deml, C., Peters, J., and Meinshausen, N. Invariant causal prediction for nonlinear models. *Journal of Causal Inference*, 2018b.
- Janzing, D. and Schölkopf, B. Causal inference using the algorithmic markov condition. *IEEE Transactions on Information Theory*, 56(10):5168–5194, 2010.
- Ke, N. R., Bilaniuk, O., Goyal, A., Bauer, S., Larochelle, H., Pal, C., and Bengio, Y. Learning neural causal models from unknown interventions. *arXiv preprint arXiv:1910.01075*, 2019.
- Mooij, J. M., Peters, J., Janzing, D., Zscheischler, J., and Schölkopf, B. Distinguishing cause from effect using observational data: Methods and benchmarks. *Journal of Machine Learning Research*, 2016.
- Nesterov, Y. *Introductory Lectures on Convex Optimization: A Basic Course*. Springer, 2004.
- Parikh, N., Boyd, S., et al. Proximal algorithms. *Foundations and Trends® in Optimization*, 1(3):127–239, 2014.
- Pearl, J. *Causality*. Cambridge university press, 2009.
- Pearl, J. and Bareinboim, E. External validity: From do-calculus to transportability across populations. *Statistical Science*, 2014.
- Peters, J., Bühlmann, P., and Meinshausen, N. Causal inference by using invariant prediction: identification and confidence intervals. *Journal of the Royal Statistical Society: Series B (Statistical Methodology)*, 2016.
- Peters, J., Janzing, D., and Schölkopf, B. *Elements of causal inference: foundations and learning algorithms*. MIT press, 2017.
- Rothenhäusler, D., Bühlmann, P., Meinshausen, N., et al. Causal dantzig: fast inference in linear structural equation models with hidden variables under additive interventions. *The Annals of Statistics*, 47(3):1688–1722, 2019.
- Schölkopf, B., Janzing, D., Peters, J., Sgouritsa, E., Zhang, K., and Mooij, J. On causal and anticausal learning. In *ICML*, 2012.
- Schölkopf, B. Causality for machine learning. *arXiv:1911.10500*, 2019.

Tian, J. and Pearl, J. Causal discovery from changes. In *UAI*, 2001.

Vapnik, V. N. and Chervonenkis, A. Y. On the uniform convergence of relative frequencies of events to their probabilities. *Soviet Mathematics Doklady*, 1971.

A. Categorical Optimization

In this section we prove a convergence rate of ASGD that applies to the categorical loss, and we show that the constants involved in this rate are the same for both causal and anticausal models.

A.1. Convergence of ASGD with Fixed Step-size

Here we derive a classical convergence rate of Average SGD. This result is standard ; we include it to be self-contained. The objective is

$$\min_{\theta} F(\theta) = \mathbb{E}_i [f(\theta, i)] .$$

Theorem A.1. *If each $f_i(\theta) = f(\theta, i)$ has bounded gradient B , then after T steps of SGD with step-size $\gamma = \frac{c}{\sqrt{T}}$, starting from θ_0 , the expected sub-optimality verifies*

$$\mathbb{E} [F(\bar{\theta}_T) - F(\theta^*)] \leq \frac{1}{2c\sqrt{T}} \|\theta_0 - \theta^*\|^2 + \frac{cB^2}{2\sqrt{T}}$$

where $\bar{\theta}_T = \frac{1}{T} \sum_t \theta_t$.

Proof. First we relate the ℓ^2 distance to optimum at step $t + 1$ with the one at step t :

$$\begin{aligned} & \|\theta_{t+1} - \theta^*\|^2 \\ &= \|\theta_t - \theta^*\|^2 - 2\gamma \langle f'_i(\theta_t), \theta_t - \theta^* \rangle + \gamma^2 \|f'_i(\theta_t)\|^2 \\ &\leq \|\theta_t - \theta^*\|^2 - 2\gamma \langle f'_i(\theta_t), \theta_t - \theta^* \rangle + \gamma^2 B^2 . \end{aligned}$$

By convexity of f_i and rearranging the terms we get

$$\begin{aligned} 2\gamma(f_i(\theta_t) - f_i(\theta^*)) &\leq 2\gamma \langle f'_i(\theta_t), \theta_t - \theta^* \rangle \\ &\leq \|\theta_t - \theta^*\|^2 - \|\theta_{t+1} - \theta^*\|^2 + \gamma^2 B^2 . \end{aligned}$$

Now we take the expectation, sum up both sides for T iterations and divide by $2T\gamma$ to get

$$\begin{aligned} & \frac{1}{T} \sum_{i=1}^T \mathbb{E} [F(\theta_t) - F(\theta^*)] \\ &\leq \frac{1}{2\gamma T} (\mathbb{E} [\|\theta_0 - \theta^*\|^2] - \mathbb{E} [\|\theta_{T+1} - \theta^*\|^2]) + \frac{\gamma B^2}{2} \\ &\leq \frac{1}{2\gamma T} \|\theta_0 - \theta^*\|^2 + \frac{\gamma B^2}{2} \end{aligned}$$

Finally, we apply Jensen inequality to F in $\bar{\theta}_T = \frac{1}{T} \sum_t \theta_t$ to get the final result. \square

A.2. Properties of the Categorical Loss

We are now going to verify that assumptions of the rate (4) apply to the negative log-likelihood loss for the categorical distribution. This loss is standard and its properties are well-known, but we review them here to be self-contained.

Each mechanism has the same form of negative log-likelihood so we simply have to check that this loss is convex, and has bounded gradients for all z . The random functions coming from sampling Z are

$$f_z(\mathbf{s}) = -s_z + \log\left(\sum_{z'} e^{s_{z'}}\right) \quad (14)$$

This function is the softmax – or logsumexp – function minus a stochastic linear term.

Convexity We are going to show that it is convex but not strongly convex because it becomes flat for large score values. Its derivative is

$$\nabla f_z(\mathbf{s}) = -\mathbf{e}_z + \mathbf{p} . \quad (15)$$

where \mathbf{e}_z is the z -th canonical basis element and \mathbf{p} is the output of the softargmax function taken on \mathbf{s}_Z . The Hessian is the same for every z .

$$\nabla^2 f_z(\mathbf{s}) = \text{diag}(\mathbf{p}) - \mathbf{p}\mathbf{p}^\top . \quad (16)$$

We observe that for any vector \mathbf{v} ,

$$\begin{aligned} \mathbf{v}^\top \nabla^2 f_z(\mathbf{s}) \mathbf{v} &= \sum_z p_z v_z^2 - \left(\sum_z p_z v_z \right)^2 \\ &= \text{Var}_{Z \sim \mathbf{p}} [v_Z] \geq 0 \end{aligned} \quad (17)$$

which means that the logsumexp is convex. When s_0 tends toward positive infinity and the other components remain constant, \mathbf{p} tends toward a dirac on the 0-th component. Then (17) is 0 for all \mathbf{v} , so the logsumexp is not strongly convex.

Bounded Gradients. By the triangular inequality, $\forall s \in \mathbb{R}^K$,

$$\|\nabla f_z(\mathbf{s})\| = \|\mathbf{p} - \mathbf{e}_z\| \quad (18)$$

$$\leq \|\mathbf{p}\| + \|\mathbf{e}_z\| \leq 2 . \quad (19)$$

The gradients are bounded by $B = 2$, or in other words, all the f_z are 2-Lipschitz. Thanks to these properties, the sample complexity of $\mathbf{p}_{\theta_{\rightarrow}}$ and $\mathbf{p}_{\theta_{\leftarrow}}$ are bounded by (4). The difference in adaptation speed between causal and anticausal models is characterized by the distance in parameter space.

A.3. Equality of Gradient Bound for Both Models

In this section we show that the stochastic gradient's norm upper bound which appears in the convergence term of ASGD in (4) denoted by B is the same for causal and anticausal models. Both marginals in causal and anticausal models have similar gradient form with different parametrizations \mathbf{s}_X , and $\mathbf{s}_Y \in \mathbb{R}^K$. Therefore to find B for each

marginal, we only need to solve the following supremum problem where s is the parameter and z is a sample

$$\sup_{z, s} \|\nabla_s f_z(s)\|^2 = \|-e_z + p(s)\|^2 \leq 2. \quad (20)$$

For s approaching infinity along axis z' , we have $p = e_{z'}$. If $z \neq z'$, then

$$\sup_{z, s} \|\nabla_s f_z(s)\|^2 \geq \|-e_z + e_{z'}\|^2 = 2.$$

which is exactly equal to the upper bound for the gradient norm in (18). With similar argument, the upper bound for the gradient magnitude of the conditional in both models is 2.

B. Categorical Analysis

In this section, we prove relationships between parameter distances induced by interventions between the causal and anticausal models. First we prove two useful lemmas. Then we establish that the causal model dominates the anticausal model by a factor K when the intervention is on the cause. Finally we show that no model has a set advantage when the intervention bears on the effect.

The logits or scores s live in \mathbb{R}^K . They have one additional degree of freedom compared to the probability p . More specifically, the softargmax is invariant by translations along the vector $\mathbf{1} = (1, \dots, 1)$. In other words, all scores $\{s + \lambda \mathbf{1} \mid \forall \lambda \in \mathbb{R}\}$ are equivalent. Scores which move by following the gradient of this loss will remain in the same affine hyperplane orthogonal to $\mathbf{1}$. To ensure that the distances we measure are meaningful, we project all logits in the hyperplane such that $\sum_z s_z = 0$, by subtracting their mean.

Definition B.1 (Mean-zero score). *A score vector s is mean-zero iff $\sum_z s_z = 0$.*

B.1. Switching Direction

In this section we are going to prove a few useful results relating cause and anticausal models. We know the causal parameters $X \rightarrow Y$, and we want to find the corresponding $X \leftarrow Y$ model, e.g. express $s_Y, s_{X|Y}$ as a function of $s_X, s_{Y|X}$. This will help us to find a relationship between δ_{causal} and $\delta_{\text{anticausal}}$. We first need to define a few useful variables

Definition B.2 (Average conditional score vectors). *For any x or y , define*

$$m(y) := \frac{1}{K} \sum_x s_{y|x}, \quad n(x) := \frac{1}{K} \sum_y s_{x|y}. \quad (21)$$

Definition B.3 (Conditional log-partition function).

$$A(x) = \log \sum_y e^{s_{y|x}} \quad (22)$$

With these variables, we can express the reverse conditional score from the causal parameters.

Lemma B.4 (Anticausal conditional score). *Let s_y, s_x be marginal scores, and $s_{y|x}, s_{x|y}$ be conditional scores. Then*

$$s_{x|y} = s_x + (s_{y|x} - m(y)) - (A(x) - \alpha), \quad (23)$$

where $\alpha = \frac{1}{K} \sum_x A(x)$.

Proof. Let's apply Bayes rule to find the conditional probability mass function

$$\begin{aligned} p(x|y) &\propto p(y|x)p(x) \\ &\propto \exp(s_{y|x} - A(x) + s_x) \end{aligned}$$

where $A(x)$ is the log-partition function of $p(y|x)$. Taking the logarithm,

$$s_{x|y} = s_x + s_{y|x} - A(x) + C(y) \quad (24)$$

where $C(y)$ is a constant defined such that $\sum_x s_{x|y} = 0$ (see Definition B.1). We take the sum of (24) over x to find

$$\begin{aligned} \sum_x s_x + \sum_x s_{y|x} - \sum_x A(x) + KC(y) \\ = 0 + Km(y) + K\alpha + KC(y) \end{aligned}$$

which simplifies into

$$C(y) = -m(y) - \alpha$$

We plug this in (24) to conclude the proof. \square

We conclude this section with an identity showing that conditional logits are equally close from their averages in both directions.

Lemma B.5. *For any x and y we have*

$$s_{x|y} - n(x) = s_{y|x} - m(y). \quad (25)$$

where $n(x) := \frac{1}{K} \sum_y s_{x|y}$ and $m(y) := \frac{1}{K} \sum_x s_{y|x}$.

Proof. We apply Lemma B.4 with the roles of X and Y inverted to express $s_{y|x}$ as a function of the anti causal parameters

$$s_{y|x} = s_y + (s_{x|y} - n(x)) - (B(y) - \beta), \quad (26)$$

where $B(y) = \log \sum_x e^{s_{y|x}}$ and $\beta = \frac{1}{K} \sum_y B(y)$. We can add (23) and (26) to get rid of the conditional scores

$$s_x - n(x) - A(x) + \alpha = -(s_y - m(y) - B(y) + \beta),$$

for all x, y . The left hand side is constant in y whereas the right hand side is constant in x . Thus both sides are

constants with respect to both x and y . In particular they are equal to their average

$$\begin{aligned} \forall x, s_x - n(x) - A(x) + \alpha &= \frac{1}{K} \sum_{x'} (s_{x'} - n(x')) \\ &\quad - \frac{1}{K} \sum_{x'} A(x') + \alpha \\ &= 0 - 0 - \alpha + \alpha \\ &= 0. \end{aligned}$$

We plug this equality into (23) to prove the lemma. \square

B.2. Intervention on the Cause

In this section, we analyze the relationship between δ_{causal} and $\delta_{\text{anticausal}}$ after an intervention on the cause.

Proposition 1. *If an intervention happens on the cause X then we have*

$$\boxed{\delta_{\text{anticausal}} \geq K \delta_{\text{causal}}}, \quad (27)$$

where $\delta_{\text{causal}} = \|\mathbf{s}_X - \mathbf{s}_X^*\|^2$, and $\delta_{\text{anticausal}} = \|\mathbf{s}_Y - \mathbf{s}_Y^*\|^2 + \sum_y \|\mathbf{s}_{X|y} - \mathbf{s}_{X|y}^*\|^2$

Proof. Given that $s_{y|x}^* = s_{y|x}$, $\mathbf{m}^* = \mathbf{m}$, $A^* = A$ and $\alpha^* = \alpha$, Lemma B.4 tells us that the anticausal conditional $\mathbf{s}_{X|Y}^*$ verifies

$$\begin{aligned} s_{x|y}^* - s_x^* &= (s_{y|x} - m(y)) - (A(x) - \alpha) = s_{x|y} - s_x \\ &\implies s_{x|y} - s_{x|y}^* = s_x - s_x^*. \end{aligned}$$

The distance between models before and after intervention are

$$\begin{aligned} \delta_{\text{causal}} &= \|\mathbf{s}_X - \mathbf{s}_X^*\|^2 \\ \delta_{\text{anticausal}} &= \|\mathbf{s}_Y - \mathbf{s}_Y^*\|^2 + \sum_y \|\mathbf{s}_{X|y} - \mathbf{s}_{X|y}^*\|^2 \\ &\geq 0 + \sum_y \sum_x (s_x - s_x^*)^2 = K \|\mathbf{s}_X - \mathbf{s}_X^*\|^2. \end{aligned}$$

In conclusion,

$$\delta_{\text{anticausal}} \geq K \delta_{\text{causal}}. \quad \square$$

B.3. Intervention on the Effect

The following proposition shows that when the intervention is on the effect, the causal model is advantaged only when the new effect marginal \mathbf{s}_Y^* is close enough from the previous marginal.

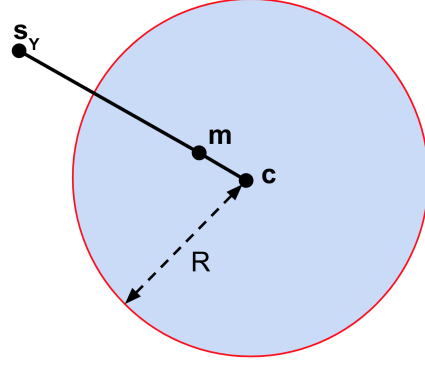


Figure 7. \mathbf{m} is a convex combination of \mathbf{c} and \mathbf{s}_Y . The red circle is the level line 0 of Δ . It is a circle of radius R centered at \mathbf{c} . Within this circle, $\delta_{\text{causal}} \leq \delta_{\text{anticausal}}$ the causal model is advantaged. Outside this circle, $\delta_{\text{causal}} \geq \delta_{\text{anticausal}}$ the anticausal model is advantaged.

Proposition 2 *When an intervention happens on the effect*

$$\Delta := \delta_{\text{causal}} - \delta_{\text{anticausal}} \quad (28)$$

$$= (K - 1) \left(\|\mathbf{s}_Y^* - \mathbf{c}\|^2 - R^2 \right) \quad (29)$$

where the score vector \mathbf{c} and the scalar R are defined as

$$\mathbf{c} = \frac{K \mathbf{m} - \mathbf{s}_Y}{K - 1} \quad (30)$$

$$\begin{aligned} (K - 1)R^2 &= K \|\mathbf{n} - \mathbf{s}_X\|^2 + (K - 1) \|\mathbf{c}\|^2 \\ &\quad + \|\mathbf{s}_Y\|^2 - K \|\mathbf{m}\|^2 \end{aligned} \quad (31)$$

with \mathbf{m} and \mathbf{n} as in Definition B.2.

We illustrate the relationship between \mathbf{m} , \mathbf{c} , \mathbf{s}_Y and R in Figure 7.

Proof. First we expand the causal distance with a bias variance decomposition

$$\begin{aligned} \delta_{\text{causal}} &= \sum_x \|\mathbf{s}_{Y|x} - \mathbf{s}_Y^*\|^2 \\ &= \sum_{x,y} (s_{y|x} - m(y) + m(y) - s_y^*)^2 \\ &= \sum_{x,y} (s_{y|x} - m(y))^2 + K \sum_y (m(y) - s_y^*)^2 \\ &\quad + 2 \sum_y (m(y) - s_y^*) \underbrace{\sum_x (s_{y|x} - m(y))}_{=0}. \end{aligned} \quad (32)$$

Given that $\mathbf{s}_{X|y}^* = \mathbf{s}_X$, we can decompose the anticausal

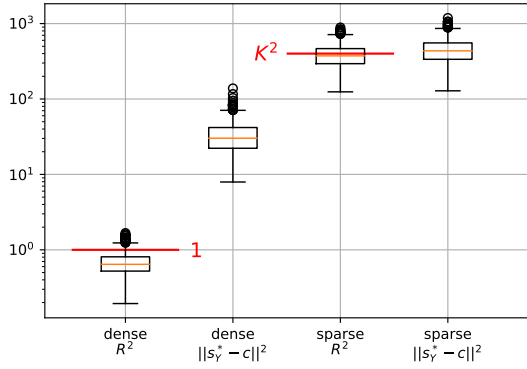


Figure 8. Box plots for the radius R^2 and deviations $\|s_Y^* - c\|^2$ for $K = 20$ with the dense prior (left) and the sparse prior (right). The y-axis is logarithmic. Red lines show analytical estimates for the expected radius.

distance similarly

$$\begin{aligned}
\delta_{\text{anticausal}} &= \|s_Y - s_Y^*\|^2 + \sum_y \|s_{X|y} - s_{X|y}^*\|^2 \\
&= \|s_Y - s_Y^*\|^2 + \sum_{x,y} (s_{x|y} - n(x) + n(x) - s_x)^2 \\
&= \|s_Y - s_Y^*\|^2 + \sum_{x,y} (s_{x|y} - n(x))^2 \\
&\quad + K \sum_x (n(x) - s_x)^2. \tag{33}
\end{aligned}$$

Thanks to Lemma B.5, the variance of conditional score vectors (in blue) in (32) and (33) are equal

$$\sum_{x,y} (s_{x|y} - n(x))^2 = \sum_{x,y} (s_{y|x} - m(y))^2.$$

What remains in the difference is the quadratic form

$$\begin{aligned}
\Delta &= \delta_{\text{causal}} - \delta_{\text{anticausal}} \\
&= K \|m - s_Y^*\|^2 - K \|n - s_X\|^2 - \|s_Y - s_Y^*\|^2,
\end{aligned}$$

which we can expand to highlight the role of s_Y^* as

$$\begin{aligned}
\Delta &= (K-1) \|s_Y^*\|^2 - 2 \langle s_Y^*, K m - s_Y \rangle \\
&\quad + K \|m\|^2 - \|s_Y\|^2 - K \|n - s_X\|^2 \\
&= (K-1) \|s_Y^* - c\|^2 - (K-1) \|c\|^2 \\
&\quad + K \|m\|^2 - \|s_Y\|^2 - K \|n - s_X\|^2
\end{aligned}$$

where c appears as a non-convex interpolation of m and s_Y , $c = \frac{K m - s_Y}{K-1}$. Define R^2 to conclude the proof. \square

Empirical estimates of the radius. We report values of R^2 and $\|s_Y^* - c\|^2$ observed for the dense and sparse priors in Figure 8. For dense prior radii are much smaller than deviations, whereas for the sparse prior they have similar magnitude. This explains why the anticausal model systematically adapts faster when the intervention is on the effect and the prior is dense. We also observe that radii (and deviations) are much greater for the sparse prior than for the dense prior. In the following paragraph we provide some clues to explain this behaviour.

As illustrated by Figure 7, m is a convex combination of c and s_Y : $m = \frac{(K-1)c + s_Y}{K}$ so by convexity of $\|\cdot\|^2$,

$$\begin{aligned}
\frac{K-1}{K} \|c\|^2 + \frac{1}{K} \|s_Y\|^2 &\geq \|m\|^2 \\
\Rightarrow (K-1) \|c\|^2 + \|s_Y\|^2 - K \|m\|^2 &\geq 0 \\
\Rightarrow R^2 &\geq \|n - s_X\|^2.
\end{aligned}$$

As K grows larger, this inequality will get closer and closer to an equality. Indeed, m will get closer and closer to c and we will end up with

$$\frac{K-1}{K} \|c\|^2 + \frac{1}{K} \|s_Y\|^2 - \|m\|^2 \ll \|n - s_X\|^2 \approx R^2.$$

Before proceeding, let us prove a simple proposition that is a direct consequence of Lemma B.4.

Proposition 3. *The squared distance between marginal score and reverse average conditional is equal to the empirical variance of the conditional log-partition function*

$$\|s_X - n\|^2 = K \widehat{\text{Var}}_X[A(X)]. \tag{34}$$

Proof. Taking the average of Lemma B.4 over y yields

$$\begin{aligned}
\frac{1}{K} \sum_y s_{x|y} &= s_x - (A(x) - \alpha) + \frac{1}{K} \sum_y (s_{y|x} - m(y)) \\
n(x) &= s_x - (A(x) - \alpha),
\end{aligned}$$

where we used the definition of $n(x)$ and the mean-zero scores. Reordering terms gives

$$s_x - n(x) = A(x) - \alpha \tag{35}$$

Recall that α is the average of $A(x)$ over x . Squaring this equation and summing over x concludes the proof. \square

Using this proposition we get that

$$\begin{aligned}
R^2 &\approx \|s_X - n\|^2 \\
&= K \widehat{\text{Var}}_X[A(X)] \\
&= K \widehat{\text{Var}}_X[\log \sum_y e^{s_{y|x}}].
\end{aligned}$$

Conditional scores $s_{y|x}$ are taking much greater values with much higher variance under the sparse prior than under the dense prior. To be clear, we sample independently pseudo-scores $\tilde{s}_{y|x}$ from exp-gamma laws, and we subtract their mean to ensure that they sum to 0 (Definition B.1). $s_{y|x} = \tilde{s}_{y|x} - \frac{1}{K} \sum_{y'} \tilde{s}_{y'|x}$. This means that

$$\log \sum_y e^{s_{y|x}} = \log \sum_y e^{\tilde{s}_{y|x}} - \frac{1}{K} \sum_y \tilde{s}_{y|x}$$

If we make the approximation that the logsumexp term and the average term are independent then

$$\begin{aligned} & \widehat{\text{Var}}_X[\log \sum_y e^{s_{y|x}}] \\ & \approx \text{Var}_{s_{y|x}}[\log \sum_y e^{s_{y|x}}] \\ & \approx \text{Var}_{\tilde{s}_{y|x}}[\log \sum_y e^{\tilde{s}_{y|x}}] + \frac{1}{K} \text{Var}_{\tilde{s}_{y|x}}[\sum_y \tilde{s}_{y|x}] \\ & = \psi^{(1)}(K\lambda) + \frac{1}{K} \psi^{(1)}(\lambda) \end{aligned}$$

where this last step uses the formula for the variance of an exp-gamma variable twice. The variance of an exponential gamma with shape parameter λ is $\psi^{(1)}(\lambda)$ where $\psi^{(1)}$ is the trigamma function. The log-sum-exp of K independent exp-gamma with scale and shape parameters (λ, ζ) is another exp-gamma with scale and shape parameters $(K\lambda, \zeta)$. Finally we get the following approximation for the squared radius

$$R^2 \approx K\psi^{(1)}(K\lambda) + \psi^{(1)}(\lambda).$$

The dense prior uses a shape parameter $\lambda = 1$ while the sparse prior uses a shape parameter $\lambda = \frac{1}{K}$. We use two approximations of the trigamma function: $\psi^{(1)}(\frac{1}{K}) \approx K^2 + \pi^2/6$ and $\psi^{(1)}(K) \approx \frac{1}{K}$ when $K \geq 10$.

$$\begin{aligned} R_{\text{dense}}^2 & \approx K\psi^{(1)}(K) + \psi^{(1)}(1) \\ & \approx 1 + \pi^2/6 = O(1) \\ R_{\text{sparse}}^2 & \approx K\psi^{(1)}(\frac{1}{K}) + \psi^{(1)}(\frac{1}{K}) \\ & \approx K^2 + K\pi^2/6 + \pi^2/6 = O(K^2). \end{aligned}$$

In other words for dense prior the radius grows linearly with the dimension K . We report these estimates along with real data in Figure 8.

Independent Special Case. if X is independent of Y in the reference distribution – e.g. $\forall x, y, p(x, y) = p(x)p(y)$ – then $\forall x, y$,

$$\begin{aligned} s_x & = s_{x|y} = n(x) \\ s_y & = s_{y|x} = m(y) \end{aligned}$$

Plugging these equalities into Proposition 2 yields

$$\begin{aligned} c & = m = s_Y \quad \text{and} \quad R = 0 \\ \implies \Delta & = (K - 1) \|s_Y^* - s_Y\|^2 \geq 0 \end{aligned}$$

which means that the anticausal model is advantaged $\delta_{\text{causal}} \geq \delta_{\text{anticausal}}$. This is actually predictable from a simple parameter counting argument. When the reference distribution is made of independent distributions, the anticausal conditional mechanism is already optimal $s_x = s_{x|y}$. The anticausal model only has to adapt its marginal mechanism s_Y of size K . On contrary, the causal model only has to adapt its conditional mechanism $s_{y|x} \neq s_y$ of size K^2 . Overall the causal model has to adapt K times more parameters than the anticausal model.

B.4. Single Mechanism Intervention

If only $s_{Y|x_0}$ changes, for some x_0 , then from Lemma B.4 we get the following equality

$$\begin{aligned} \delta_{\text{anticausal}} & = \frac{K-1}{K} \delta_{\text{causal}} + \|s_Y^* - s_Y\|^2 \\ & \quad + (K-1)(A^*(x_0) - A(x_0))^2. \end{aligned} \quad (36)$$

The causal and anticausal distances seem to be on the same scale, with a multiplicative factor $\frac{K-1}{K} \lesssim 1$ and a positive additive factor. This is interesting because the sparsity argument holds: the causal model needs to change K parameters whereas the anticausal model needs to change $K^2 + K$ parameters. That means we could expect an advantage by a factor K for the causal model, similarly to when the intervention is on the cause. However (36) tells another story: without further assumptions, it seems like both distances will have the same scale.

Experiments. For this kind of intervention to be detectable, we need to intervene on x_0 such that $p(x_0)$ is quite large. To ensure this in our experiments, we pick $x_0 = \text{argmax}_x p(x)$. We report results on dense and sparse priors in Figure 9. We observe no significant advantage for the causal model, in spite of the parameter counting prediction.

C. Categorical Priors

In this section we study the dense and sparse prior described in the main paper.

C.1. The Causal Direction is Identifiable under the Dense Prior

Chalupka et al. (2016) study the prediction of causal direction from observational data under the dense prior assumption. The causal direction $X \rightarrow Y$ induces a certain prior

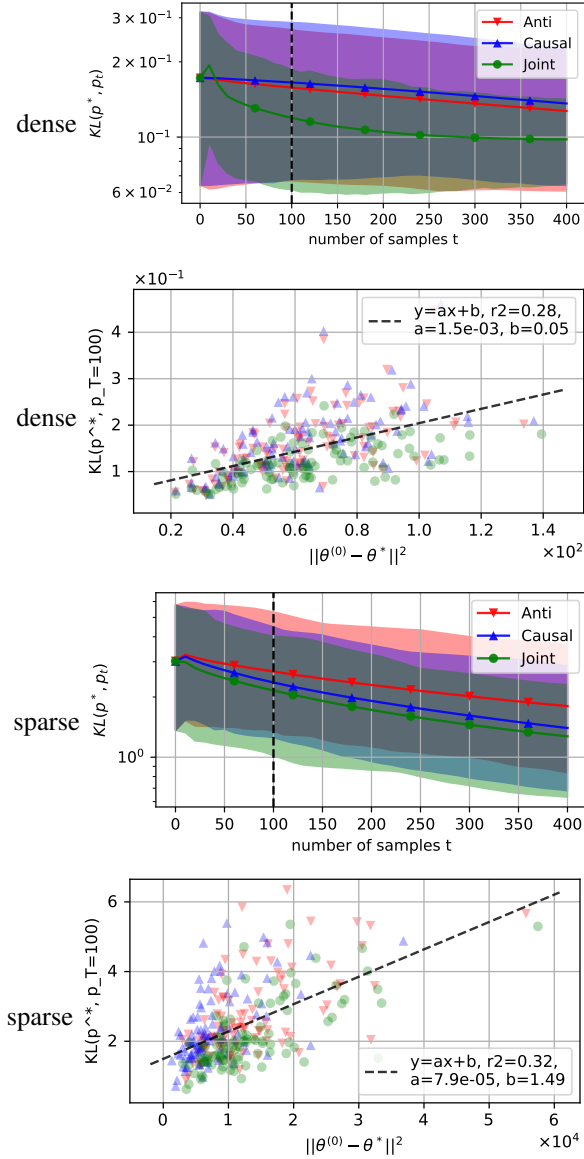


Figure 9. **Single mechanism intervention with $K=20$.** Two first rows: Dense prior. The only model to be slightly advantaged is the joint model. Two last rows: Sparse prior. This time there is a slight advantage for the causal model which performs comparably to the joint model. Overall the optimization is hard in both settings, since we are observing only K^2 samples for models with $O(K^2)$ parameters. The KL barely decreases.

over joint distributions $\pi(\mathbf{p} | \rightarrow)$. The anticausal direction $X \leftarrow Y$ induces another one $\pi(\mathbf{p} | \leftarrow)$. The Bayes classifier is predicting \rightarrow if

$$\log \pi(\rightarrow | \mathbf{p}) - \log \pi(\leftarrow | \mathbf{p}) > 0, \quad (37)$$

and \leftarrow otherwise. Under the dense prior assumption, this classifier makes an error of approximately 0.4 for $K = 2$, which decreases exponentially to 0.001 for $K = 10$. We reproduced their setting and report the error of the optimal classifier in Table 1 for varying K . In other words the dense prior induce very asymmetric distributions which makes the causal direction identifiable.

Is this Bayes classifier easy to estimate? It turns out that under the dense prior, the criterion (37) can be simplified into the following criterion

$$D_{\text{KL}}(\mathbf{u} | \mathbf{p}_X) - D_{\text{KL}}(\mathbf{u} | \mathbf{p}_Y) > 0 \quad (38)$$

where $\mathbf{u} := \mathbf{1}/K$ is the uniform probability vector. The proof is left as an exercise to the reader. If (38) is positive, Bayes predicts that the cause is X , otherwise Y is the cause. In words, whichever variable has the most uniform marginal is the effect. This simple rule is optimal given the prior assumption (and if both directions are equally likely). We can understand it from a concentration of measure perspective. The effect marginal is written as a sum of quasi independent uniform variables

$$\mathbf{p}(y) = \sum_x \mathbf{p}(y|x)\mathbf{p}(x)$$

which ends up close from the uniform vector.

C.2. Joint Distribution with Sparse Prior

The following theorem shows how a Dirichlet prior over joint distributions $c_{x,y} = \mathbf{p}(x,y)$ is equal to independent Dirichlet priors over marginal $a_x = \mathbf{p}(x)$ and conditional $b_{y|x} = \mathbf{p}(y|x)$ probability mass functions. By applying this theorem, we find that the sparse prior is equivalent to $\text{Dir}(\frac{1}{K} \mathbf{1}_{K^2})$.

Theorem C.1 (Dirichlet and Factorization). *Let \mathbf{c} be a random square matrix of dimension K . Let's define \mathbf{a} as the random vector obtained by summing columns of \mathbf{c} , and \mathbf{b} as a copy of \mathbf{c} with rows normalized so that they sum to 1. $\forall (i,j) \in \{1, \dots, K\}^2$*

$$a_i = \sum_j c_{i,j} \quad (39)$$

$$b_{j|i} = \frac{c_{i,j}}{a_i}. \quad (40)$$

Let γ be a positive square matrix of parameters. The follow-

K	2	3	4	5	6	7	8	9	10	11	12	13	14
error	.4	.2	.1	.07	.03	.01	.005	.002	.0007	.0003	7e-5	3e-5	4e-6

Table 1. Estimation of the Bayes error under the dense prior assumption for increasing categorical variables dimension K . We estimated these numbers by sampling one million joint distributions for each K . We report 1 significant figure.

ing equivalence holds

$$\mathbf{c} \sim \text{Dir}(\gamma) \iff \begin{cases} \mathbf{a} \sim \text{Dir}(\sum_i \gamma_i) \\ \mathbf{b}_{:|i} \sim \text{Dir}(\gamma_{i,:}), \forall i \\ \mathbf{a} \perp \mathbf{b}_{:|i} \perp \mathbf{b}_{:|i'}, \forall i \neq i' \end{cases} \quad (41)$$

Proof. First let's remark that the right side of (41) is entirely characterizing the joint distribution on (\mathbf{a}, \mathbf{b}) , and that the relationship between \mathbf{c} and (\mathbf{a}, \mathbf{b}) is a bijection with reverse $c_{i,j} = b_{j|i} a_i$. This means that the equivalence (41) is an equality between distributions. This means that we can prove the forward implication and the converse will hold automatically.

If $\mathbf{c} \sim \text{Dir}(\gamma)$, then there exist K^2 independent Gamma variables $\tilde{c}_{i,j} \sim \Gamma(\gamma_{i,j}, 1), \forall i, j$ such that

$$\mathbf{c} = \frac{\tilde{\mathbf{c}}}{S} \quad \text{where} \quad S = \sum_{i,j} \tilde{c}_{i,j}. \quad (42)$$

We know from properties of the Gamma distribution that \mathbf{c} is independent of S . Now let's define $\tilde{a}_i := \sum_j \tilde{c}_{i,j}$. This definition has three consequences. First \tilde{a}_i is a sum of independent gammas, so it is a gamma with parameters $(\alpha_i := \sum_j \gamma_{i,j}, 1)$. Second $S = \sum_i \tilde{a}_i$. Third $\mathbf{a} = \frac{\tilde{\mathbf{a}}}{S}$ is independent of S and is a Dirichlet with parameter vector $\boldsymbol{\alpha} = \sum_j \gamma_{:,j}$.

That was for the marginal. Now for the conditional,

$$b_{j|i} = \frac{c_{i,j}}{a_i} = \frac{\tilde{c}_{i,j}/S}{\tilde{a}_i/S} = \frac{\tilde{c}_{i,j}}{\tilde{a}_i}. \quad (43)$$

Again from properties of the Gamma distribution, $\mathbf{b}_{:|i} \perp \tilde{a}_i, \forall i$, and $\mathbf{b}_{:|i} \sim \text{Dir}(\gamma_{i,:})$. Each of the conditional $\mathbf{b}_{:|i}$ is defined with independent gammas, so we also have the independence between conditionals. We verified all properties of the right side of (41), which concludes the proof. \square

C.3. Categorical Sparse Prior Explosion

In this section we explain why the KL takes large values with sparse prior and effect intervention.

On one hand the sparse prior samples probability vectors which are close from being Dirac. On the other hand the effect intervention creates an outer product between two samples drawn uniformly from the simplex $\text{Dir}(\mathbf{1})$.

For instance, for the uniform probability vector $\mathbf{u} = \frac{1}{K^2} \mathbf{1} \in \Delta_{K^2}$ and an almost Dirac $\mathbf{p} = (1 - \varepsilon)\mathbf{e}_1 + \varepsilon\mathbf{u}$

$$D_{\text{KL}}(\mathbf{u}||\mathbf{p}) \in \Theta(\log(\frac{1}{\varepsilon}))$$

where ε is a small value. As we increase K , the sparse prior $\text{Dir}(\mathbf{1}_{K^2}/K)$ becomes more sparse. Conceptually, the value of ε decreases, and the value of $D_{\text{KL}}(\mathbf{u}||\mathbf{p})$ explodes. This is why we observe high KL values for sparse prior and effect intervention. Empirically, these values also increase with K .

D. Normal Optimization

In this Section we adapt the stochastic composite mirror-prox algorithm to our setting of unbounded multivariate normal optimization. First we describe the algorithm and prove a novel convergence rate that applies to our setting. Then we explicit the update formulas for the normal log-likelihood loss with Cholesky parameters. Finally we prove that worst case constants appearing in the rate are equal for both causal and anticausal models.

D.1. Stochastic Composite Mirror-Prox

We want to minimize the composite objective

$$F(\theta) = \mathbb{E}_i [f(\theta, i)] + g(\theta).$$

For simplicity we denote $f(\theta, i)$ by $f_i(\theta)$ and $f(\theta) = \mathbb{E}_i [f_i(\theta)]$. We assume that f_i is convex, ∇f_i is L -Lipschitz and g is a convex function. The stochastic mirror-prox algorithm update rule at time t is

$$\nu_t = \theta_{t+1} - \gamma_t f'_i(\theta_t) \quad (44)$$

$$\theta_{t+1} = \underset{\theta}{\text{argmin}} \left\{ g(\theta) + \frac{1}{\gamma_t} \mathcal{B}_h(\theta, \nu_t) \right\} \quad (45)$$

where f_i is sampled randomly. $B_h(x, y) = h(x) - h(y) - \langle h'(y), x - y \rangle$ denotes the Bregman divergence between x and y induced by the convex function h and we have $\|B_h(x, y)\| \geq \frac{\alpha}{2} \|x - y\|^2$. When we set $h(x) = 1/2 \|x\|^2$, we recover something called the proximal stochastic gradient method (Duchi & Singer, 2009), also known as Perturbed proximal gradient algorithm (Atchadé et al., 2017). This last citation in particular has hypothesis very close to ours.

D.1.1. CONVERGENCE RATE

The following Theorem is a mild modification of the Theorem 8 in (Duchi et al., 2010). Our result is different in 2 ways. First, we remove the boundedness assumption for the Bregman divergence throughout the trajectory i.e. $\mathcal{B}_h(\theta^*, \theta_t) \leq D$ for all t . Second, we replace the f_i B -Lipschitz continuous assumption by ∇f_i B -Lipschitz continuous. We need this last modification for the result to hold on f_i quadratic.

First we prove the following lemma which is a modification of Lemma 1 in (Duchi et al., 2010).

Lemma D.1. *With the above assumption on f and g and $\gamma \leq \frac{\alpha}{3B}$, at iteration t , if we sample i , we have:*

$$\gamma \{f_i(\theta_t) + g(\theta_{t+1}) - F(\theta^*)\} \leq \mathcal{B}_h(\theta^*, \theta_t) - \mathcal{B}_h(\theta^*, \theta_{t+1}) + \gamma \{f_i(\theta_t) - f_i(\theta_{t+1})\}.$$

Proof. We have the following sequence of inequality

$$\begin{aligned} & \gamma \left(f_i(\theta_t) + g(\theta_{t+1}) - F(\theta^*) \right) \\ & \leq \gamma \langle \theta_t - \theta^*, f'_i(\theta_t) \rangle + \gamma \langle \theta_{t+1} - \theta^*, \partial g_t(\theta_t) \rangle \\ & \leq \mathcal{B}_h(\theta^*, \theta_t) - \mathcal{B}_h(\theta^*, \theta_{t+1}) \\ & \quad - \mathcal{B}_h(\theta_{t+1}, \theta_t) + \gamma \langle \theta_t - \theta_{t+1}, f'_i(\theta_t) \rangle \\ & \leq \mathcal{B}_h(\theta^*, \theta_t) - \mathcal{B}_h(\theta^*, \theta_{t+1}) \\ & \quad - \mathcal{B}_h(\theta_{t+1}, \theta_t) + \frac{B\gamma}{2} \|\theta_t - \theta_{t+1}\|^2 \\ & \quad + \gamma \left(f_i(\theta_t) - f_i(\theta_{t+1}) \right) \end{aligned}$$

where the first inequality comes from convexity of f_i and g , the second inequality comes from Eq.(6) of lemma 1 in (Duchi et al., 2010), and the third inequality comes from the smoothness of f_i . By $\gamma \leq \frac{\alpha}{3L}$, the term $-\mathcal{B}_h(\theta_{t+1}, \theta_t) + \frac{B\gamma}{2} \|\theta_t - \theta_{t+1}\|^2$ is negative: we can drop this term and get the required result. Note that ∂g is a subgradient of g . \square

Theorem D.2. *Given the above assumptions for f_i and g , after T iterations of the stochastic mirror prox algorithm with $\gamma = \frac{c}{\sqrt{T}}$, ($c \leq \frac{\alpha}{3B}$), we have*

$$\mathbb{E} [F(\bar{\theta}) - F(\theta^*)] \leq \frac{\mathcal{B}_h(\theta^*, \theta_0)}{c\sqrt{T}} + \frac{(F(\theta_0) - F(\theta^*))}{T}.$$

Proof. The proof is similar to the proof of the Theorem 8 in (Duchi et al., 2010) with some modifications. Take the expectation of lemma D.1 with respect to the samples $(i_u)_{u \leq t}$

$$\begin{aligned} & \mathbb{E} \left[\gamma \left(f(\theta_t) + g(\theta_{t+1}) - F(\theta^*) \right) \right] \\ & \leq \mathbb{E} \left[\mathcal{B}_h(\theta^*, \theta_t) - \mathcal{B}_h(\theta^*, \theta_{t+1}) + \gamma \left(f(\theta_t) - f(\theta_{t+1}) \right) \right] \end{aligned}$$

where θ_t and θ_{t+1} are random variable that depends on the samples. Sum up both side for T iterations:

$$\begin{aligned} & \gamma \sum_{t=0}^T \mathbb{E} [f(\theta_t) + g(\theta_{t+1}) - F(\theta^*)] \\ & \leq \mathcal{B}_h(\theta^*, \theta_0) - \mathbb{E} [\mathcal{B}_h(\theta^*, \theta_{T+1})] \\ & \quad + \gamma \left(f(\theta_0) - \mathbb{E} [f(\theta_{T+1})] \right) \end{aligned}$$

By adding $\gamma \mathbb{E} [g(\theta_0) - g(\theta_{t+1})]$ to both sides of the above inequality we get:

$$\begin{aligned} & \gamma \sum_{t=1}^T \mathbb{E} [F(\theta_t) - F(\theta^*)] \\ & \leq \mathcal{B}_h(\theta^*, \theta_0) - \mathbb{E} [\mathcal{B}_h(\theta^*, \theta_{T+1})] \\ & \quad + \gamma \left(F(\theta_0) - \mathbb{E} [F(\theta_{T+1})] \right) \\ & \leq \mathcal{B}_h(\theta^*, \theta_0) + \gamma \left(F(\theta_0) - \mathbb{E} [F(\theta^*)] \right) \end{aligned}$$

where the last inequality is due to non-negativity of Bregman divergence and optimality of θ^* . Divide both sides by $\gamma T = c\sqrt{T}$ and use Jensen nequality on F to conclude the proof. \square

D.2. Updates for the Normal Case

The objective function at hand is:

$$F(L, \zeta) = f(L, \zeta) + g(L)$$

$$f(L, \zeta) = \frac{1}{2n} \sum_{i=1}^n \|L^T x_i - \zeta\|^2$$

$$g(L) = -\ln(|L|).$$

Now the update rule for the ζ given that g is independent of ζ and we sample mini-batch B of size m :

$$\zeta_{t+1} = (1 - \gamma)\zeta_t + \gamma L_t^T \left(\frac{1}{m} \sum_{i \in B} x_i \right)$$

For the L the gradient update gives

$$L_{t+\frac{1}{2}} = L_t - \gamma \frac{1}{m} \sum_{i \in B} (x_i x_i^T L_t - x_i \zeta_t^T).$$

Since L is lower triangular, $g(L) = \ln(|L|) = \sum_{i=1}^d \log L_{i,i}$ and the proximal operator only applies to diagonal elements of L - e.g. when $i \neq j$ $[L_{t+1}]_{(i,j)} = [L_{t+\frac{1}{2}}]_{(i,j)}$. Otherwise we have to compute:

$$[L_{t+1}]_{(i,i)} = \operatorname{argmin}_{L_{ii}} \left\{ -\ln(L_{ii}) + \frac{1}{2\gamma} \|L_{ii} - [L_{t+\frac{1}{2}}]_{(i,i)}\|^2 \right\}.$$

Therefore the update rule for the $[L_{t+1}]_{(i,i)}$ is:

$$[L_{t+1}]_{(i,i)} = \frac{1}{2} \left\{ [L_{t+\frac{1}{2}}]_{(i,i)} + \sqrt{[L_{t+\frac{1}{2}}]_{(i,i)}^2 + 4\gamma} \right\}.$$

Remark how this proximal operator behaves as a smooth projection on the set of strictly positive numbers. If the diagonal is negative after the gradient update, it brings it to a small positive value. If it was already positive, it slightly increases its value.

D.3. Equality of Smoothness Constants

In this section, we show that the Lipschitz smoothness parameter B , which appears in the convergence rate (12), is the same for both causal and anticausal models. Similarly to the categorical case, we reason about marginals loss first because they have a simpler form.

The loss of a marginal mechanism is $f_x(L, \zeta) = \frac{1}{2} \sum_{i=1}^d (\zeta_i - L_i^T x)^2$ where x is a sample observation and the L_i are the columns of L . We need to show that its Hessian is upper-bounded $\|\nabla^2 f_x(L, \zeta)\| \leq B$. Thanks to the objective f_x being quadratic, the Hessian is independent of the parameters (L, ζ) . It depends only on the data x . Since the data domain is *a priori* the same for causal and anticausal models – e.g. X and Y can live in the same range – the upper bound for the Hessian is the same. This holds true at least for marginal mechanisms, because their loss is written exactly like above.

For conditional mechanisms, this is a bit more complicated but the reasoning holds. The objective is similar, with extra parameters coming from the linear relationship between X and Y . The Cholesky parametrization is described in equation (53). The conditional model uses $\zeta_{Y|X} = MX + m$ where M is a matrix, m is a vector and X is a given sample. This means that the objective is still a quadratic and that 2nd order derivatives w.r.t. $L_{Y|X}$ are still independent of the parameters M and m . They depend only on the observed values of X and Y . We assume that these variables have the same domain *a priori*, therefore both models have similar worst case smoothness constants.

E. Normal Analysis

In this section we introduce three different parametrization of the multivariate normal cause-effect model. The mean parametrization is the most common and intuitive, but it yields a non-convex optimization problem. The natural parametrization yields a convex problem with convergence guarantees, but it has no closed update formulas for our optimization algorithm of choice. The Cholesky parametrization offers both a convex problem and simple updates.

Then we proceed to study how interventions induce distance in parameter space. We prove that in the natural parameter

space, an intervention on the cause will create more distance in the anticausal model than in the causal model.

E.1. Mean Parameters

Cause X and effect Y are sampled from the causal model

$$\begin{aligned} X &\sim \mathcal{N}(\mu_X, \Sigma_X) \\ Y|X &\sim \mathcal{N}(AX + a, \Sigma_{Y|X}) \end{aligned}$$

with parameters $(\mu_X, \Sigma_X, A, a, \Sigma_{Y|X})$. All along, we will assume that all normal laws are non-degenerate – e.g. $\Sigma_X > 0, \Sigma_{Y|X} > 0$. We compute the marginal mean and covariance of Y as well as the covariance between X and Y

$$\begin{aligned} \mathbb{E}[Y] &= A\mu_X + a \\ \text{Cov}[Y] &= \Sigma_{Y|X} + A\Sigma_X A^\top \\ \text{Cov}[X, Y] &= \Sigma_X A^\top. \end{aligned}$$

From there we can derive the joint distribution as a function of the causal parameters

$$\begin{pmatrix} X \\ Y \end{pmatrix} \sim \mathcal{N} \left(\begin{pmatrix} \mu_X \\ A\mu_X + a \end{pmatrix}, \begin{pmatrix} \Sigma_X & \Sigma_X A^\top \\ A\Sigma_X & \Sigma_{Y|X} + A\Sigma_X A^\top \end{pmatrix} \right).$$

E.2. Natural Parameters

We want the negative log-likelihood objective to be convex, so we are going to use the natural parameters instead of the mean parameters

$$\mathcal{N}(\mu, \Sigma) = \mathcal{N}_{\text{nat}}(\eta = \Sigma^{-1}\mu, \Lambda = \Sigma^{-1})$$

where we are using \mathcal{N}_{nat} to explicit that this is taking the natural parameters as arguments. Our causal model using natural parameters is:

$$\begin{aligned} X &\sim \mathcal{N}_{\text{nat}}(\eta_X, \Lambda_X) \\ Y|X &\sim \mathcal{N}_{\text{nat}}(BX + b, \Lambda_{Y|X}) \end{aligned} \quad (46)$$

where we get the natural parameters from the mean parameters with formulas

$$\begin{aligned} \Lambda_X &= \Sigma_X^{-1} \\ \Lambda_{Y|X} &= \Sigma_{Y|X}^{-1} \\ \eta_X &= \Lambda_X \mu_X \\ B &= \Lambda_{Y|X} A \\ b &= \Lambda_{Y|X} a \end{aligned}$$

E.2.1. SWITCHING DIRECTION

We want to get the natural parameters of the anticausal model as a function of the causal parameters. To do so we are going to express the natural parameters of the joint,

and then we will simply have to swap rows and columns to invert the roles of X and Y . To get the joint precision matrix, we need to invert the joint covariance. We use the Schur complement and the blockwise matrix inversion formulas

$$\begin{aligned} M &= \begin{pmatrix} A & B \\ C & D \end{pmatrix} \\ M/D &:= D - CA^{-1}B \\ M^{-1} &= \\ &\begin{pmatrix} A^{-1} + A^{-1}B(M/D)^{-1}CA^{-1} & -A^{-1}B(M/D)^{-1} \\ (M/D)^{-1}CA^{-1} & (M/D)^{-1} \end{pmatrix} \end{aligned}$$

In our case, the Schur complement of Σ with respect to its lower right block Σ_Y is precisely

$$\begin{aligned} M/D &= \Sigma/\Sigma_Y \\ &= \Sigma_{Y|X} + A\Sigma_X A^\top - A\Sigma_X \Sigma_X^{-1} \Sigma_X A^\top \\ &= \Sigma_{Y|X}. \end{aligned}$$

By applying the formula and identifying the natural parameters, we get

$$\Lambda = \begin{pmatrix} \Lambda_X + B^\top \Lambda_{Y|X}^{-1} B & -B^\top \\ -B & \Lambda_{Y|X} \end{pmatrix}$$

To get the first natural parameter, all we have to do is to multiply the joint precision and the joint mean

$$\begin{aligned} \eta &= \Lambda \mu \\ &= \begin{pmatrix} \Lambda_X \mu_X + B^\top \Lambda_{Y|X}^{-1} B \mu_X - B^\top A \mu_X - B^\top a \\ -B \mu_X + \Lambda_{Y|X} A \mu_X + \Lambda_{Y|X} a \end{pmatrix} \\ &= \begin{pmatrix} \eta_X - B^\top \Lambda_{Y|X}^{-1} b \\ b \end{pmatrix} \end{aligned}$$

where $B^\top \Lambda_{Y|X}^{-1} B \mu_X - B^\top A \mu_X$, and $-B \mu_X + \Lambda_{Y|X} A \mu_X$ are zero and we express the other terms with natural parameters. Overall, the joint natural parameters are

$$\mathcal{N}_{\text{nat}} \left(\begin{pmatrix} \eta_X - B^\top \Lambda_{Y|X}^{-1} b \\ b \end{pmatrix}, \begin{pmatrix} \Lambda_X + B^\top \Lambda_{Y|X}^{-1} B & -B^\top \\ -B & \Lambda_{Y|X} \end{pmatrix} \right).$$

From there we can use a symmetry argument to switch from causal $X \rightarrow Y$ to anticausal $X \leftarrow Y$ model.

$$\begin{aligned} Y &\sim \mathcal{N}_{\text{nat}}(\eta_Y, \Lambda_Y) \\ X|Y &\sim \mathcal{N}_{\text{nat}}(CY + c, \Lambda_{X|Y}) \end{aligned}$$

with the following formulas for the conditional mechanism

$$C = B^\top \quad (47)$$

$$c = \eta_X - B^\top \Lambda_{Y|X}^{-1} b \quad (48)$$

$$\Lambda_{X|Y} = \Lambda_X + B^\top \Lambda_{Y|X}^{-1} B \quad (49)$$

followed by these formulas for the marginal mechanisms

$$\Lambda_Y + C^\top \Lambda_{X|Y}^{-1} C = \Lambda_{Y|X} \quad (50)$$

$$\eta_Y - C^\top \Lambda_{X|Y}^{-1} c = b. \quad (51)$$

These formulas are going to be very useful to establish a relationship between the distance to optimum of the causal and anticausal models in Appendix E.5.

E.3. Cholesky Parameters

We call Cholesky parametrization of the normal law the parameters (\mathbf{L}, ζ) such that

$$\begin{aligned} \Lambda &= \mathbf{L}\mathbf{L}^\top \quad (\mathbf{L} \text{ is lower triangular}) \\ \zeta &= \mathbf{L}^{-1}\eta = \mathbf{L}^\top \mu \end{aligned}$$

We use $\mathcal{N}_{\text{cho}}(\zeta, \mathbf{L})$ to denote the normal law with Cholesky parameters ζ and \mathbf{L} . The full causal model (46) becomes

$$\begin{aligned} X &\sim \mathcal{N}_{\text{cho}}(\zeta_X, \mathbf{L}_X) \\ Y|X &\sim \mathcal{N}_{\text{cho}}(MX + m, \mathbf{L}_{Y|X}) \end{aligned} \quad (52)$$

where the 5 parameters are defined from the natural model by the equations

$$\begin{aligned} \mathbf{L}_X \mathbf{L}_X^\top &= \Lambda_X \\ \mathbf{L}_{Y|X} \mathbf{L}_{Y|X}^\top &= \Lambda_{Y|X} \\ \zeta_X &= \mathbf{L}_X^{-1} \eta_X \\ M &= \mathbf{L}_{Y|X}^{-1} B \\ m &= \mathbf{L}_{Y|X}^{-1} b \end{aligned} \quad (53)$$

There is no closed formula to express the Cholesky decomposition of a sum of matrix $A + B$ with the Cholesky decomposition of A and B . As a consequence, there is no simple formula to switch between causal and anticausal models with this parametrization.

E.3.1. JOINT CHOLESKY

We derive a formula for the joint Cholesky for future reference. To get a closed form for the joint Cholesky parameters from the conditional parameters, we need to switch the positions of X and Y in the joint vector – e.g. we are using (Y, X) instead of (X, Y) . Indeed the Cholesky decomposition is very dependent on the orders of the rows and columns. That's also why we cannot simply switch the column orders in the joint representation.

$$\begin{pmatrix} Y \\ X \end{pmatrix} \sim \mathcal{N}_{\text{cho}} \left(\begin{pmatrix} m \\ \zeta_X \end{pmatrix}, \begin{pmatrix} \mathbf{L}_{Y|X} & 0 \\ -M^\top & \mathbf{L}_X \end{pmatrix} \right).$$

This joint representation is simply taking the conditional parameters and putting them in an array. It has the advantage

that the distance is equal to the conditional distance. It hints towards the idea that for multivariate normal variables, knowing the right Cholesky decomposition is equivalent to knowing the right causal graph.

E.4. Kullback Leibler Divergence

We express the KL divergence in all three parametrizations because we use them in the code.

$$\begin{aligned}
2D_{\text{KL}}(\mathcal{N}_0||\mathcal{N}_1) &= (\mu_1 - \mu_0)^\top \Sigma_1^{-1} (\mu_1 - \mu_0) \\
&\quad + \text{Tr}(\Sigma_1^{-1} \Sigma_0) - k - \log|\Sigma_1^{-1} \Sigma_0| \\
&= \eta_1^\top \Lambda_1^{-1} \eta_1 - 2\eta_1^\top \Lambda_0^{-1} \eta_0 + \eta_0^\top \Lambda_0^{-1} \Lambda_1 \Lambda_0^{-1} \eta_0 \\
&\quad + \text{Tr}(\Lambda_1 \Lambda_0^{-1}) - k - \log|\Lambda_1 \Lambda_0^{-1}| \\
&= \|V^\top \zeta_0 - \zeta_1\|^2 + \|V\|_F^2 - k - 2\log|V|
\end{aligned}$$

where $V := \mathbf{L}_0^{-1} \mathbf{L}_1$ is a lower triangular matrix which plays a special role.

E.5. Distance after Interventions

In this section we evaluate the effect on interventions on the cause and effect for both models. When the intervention happens on the cause, we replace μ_X, Σ_X by $\tilde{\mu}_X, \tilde{\Sigma}_X$, or equivalently we replace the natural parameters of the marginal on X . The natural causal distance is simply

$$\delta_{\text{causal}} = \|\eta_X - \tilde{\eta}_X\|^2 + \|\Lambda_X - \tilde{\Lambda}_X\|_F^2.$$

Unless indicated otherwise, we will consider the Frobenius distance between matrices. For the anticausal model, both marginal and conditional parameters need to change. Here similar to categorical case, we have

$$\delta_{\text{anticausal}} \geq \delta_{\text{causal}}.$$

However when the intervention happens on the effect, there is no clear formal relation between δ_{causal} and $\delta_{\text{anticausal}}$. More detail about the deriving the mathematical formula for δ_{causal} and $\delta_{\text{anticausal}}$ is presented in the following.

E.5.1. INTERVENTION ON CAUSE

When the intervention happens on the cause, the natural causal distance is

$$\delta_{\text{causal}} = \|\eta_X - \tilde{\eta}_X\|^2 + \|\Lambda_X - \tilde{\Lambda}_X\|_F^2.$$

How does this transformation affect the anticausal parameters? Both the marginal and the conditional have to adapt. The anticausal conditional is elegantly expressed with the causal natural parameters in (49), so we will start with the

conditional

$$C - \tilde{C} = B^\top - \tilde{B}^\top = 0 \quad (54)$$

$$c - \tilde{c} = \eta_X - \tilde{\eta}_X \quad (55)$$

$$\Lambda_{X|Y} - \tilde{\Lambda}_{X|Y} = \Lambda_X - \tilde{\Lambda}_X. \quad (56)$$

In words, the linear transformation is invariant, the bias moves like the mean of X , and the conditional precision moves like the precision of X . This means that we can directly lower bound the anticausal distance with the causal distance

$$\begin{aligned}
\delta_{\text{anticausal}} &= \|C - \tilde{C}\|^2 + \|c - \tilde{c}\|^2 + \|\Lambda_{X|Y} - \tilde{\Lambda}_{X|Y}\|^2 \\
&\quad + \|\Lambda_Y - \tilde{\Lambda}_Y\|^2 + \|\eta_Y - \tilde{\eta}_Y\|^2 \\
&= \delta_{\text{causal}} + \|\Lambda_Y - \tilde{\Lambda}_Y\|^2 + \|\eta_Y - \tilde{\eta}_Y\|^2 \\
&> \delta_{\text{causal}}.
\end{aligned} \quad (57)$$

We could get a stronger bound by bounding the anticausal marginal parameters, but any such bound would involve the value of the linearity B and make the result needlessly more complicated.

E.5.2. INTERVENTION ON EFFECT

We perform an intervention on Y such that the causal model become independent

$$\begin{aligned}
X &\sim \mathcal{N}(\mu_X, \Sigma_X) \\
Y &\sim \mathcal{N}(\tilde{\mu}_Y, \tilde{\Sigma}_Y).
\end{aligned}$$

This independence means that the linear models have a slope 0

$$\tilde{A} = \tilde{B} = \tilde{C} = 0.$$

The bias then has to account for the mean parameter

$$\tilde{a} = \tilde{\mu}_Y, \quad \tilde{b} = \tilde{\eta}_Y, \quad \tilde{c} = \eta_X$$

And the conditional precision have to match the marginal precision

$$\tilde{\Sigma}_{Y|X} = \tilde{\Sigma}_Y, \quad \tilde{\Lambda}_{Y|X} = \tilde{\Lambda}_Y, \quad \tilde{\Lambda}_{X|Y} = \Lambda_X$$

So the distances are written

$$\begin{aligned}
\delta_{\text{causal}} &= \|B\|_F^2 + \|b - \tilde{\eta}_Y\|^2 + \|\Lambda_{Y|X} - \tilde{\Lambda}_Y\|_F^2 \\
\delta_{\text{anticausal}} &= \|C\|_F^2 + \|c - \eta_X\|^2 + \|\Lambda_{X|Y} - \Lambda_X\|_F^2 \\
&\quad + \|\eta_Y - \tilde{\eta}_Y\|^2 + \|\Lambda_Y - \tilde{\Lambda}_Y\|_F^2 \\
&= \|B\|_F^2 + \|B^\top \Lambda_{Y|X}^{-1} b\|^2 + \|B^\top \Lambda_{Y|X}^{-1} B\|_F^2 \\
&\quad + \|\eta_Y - \tilde{\eta}_Y\|^2 + \|\Lambda_Y - \tilde{\Lambda}_Y\|_F^2
\end{aligned}$$

We did not find any meaningful simplification of these formulas.

F. Normal Prior

Exactly like in the categorical setting, the distributions we sample are going to impact the speed of adaptation and the distances we measure. Let K be the dimension of X and Y , and $n_0 = 2K + 2$ an arbitrary number of prior observations. We define a *pseudo-conjugate prior*

$$\Lambda_X \sim \mathcal{W}(n_0, \frac{I_K}{K}) \quad (58)$$

$$\eta_X | \Lambda_X \sim \mathcal{N}(0, \frac{\Lambda_X}{n_0}) \quad (59)$$

$$\Lambda_{Y|X} \sim \mathcal{W}(n_0, 10 \frac{I_K}{K}) \quad (60)$$

$$b | \Lambda_{Y|X} \sim \mathcal{N}(0, \frac{\Lambda_{Y|X}}{n_0}) \quad (61)$$

$$B = \Lambda_{Y|X} A \text{ where } A \sim \mathcal{N}(0, \frac{I_{K^2}}{\sqrt{K}}) \quad (62)$$

where \mathcal{W} is the Wishart distribution with parameters: degrees of freedom and scale matrix. We picked these parameters such that η_Y, Λ_Y follows approximately the same law as η_X, Λ_X . Two important factors to get a symmetric relationship between X and Y are **10** and \sqrt{K} . First, we sample a larger conditional precision, so that their relationship is quite deterministic. Second we sample the linear layer such that it preserves the scale of X , so that X and Y have approximately the same variance. We also use appropriate covariance matrices to sample other parameters such that the prior is somewhat conjugate and gives proper variance formulas.

We sample interventions from the same distributions as the cause marginal in (62). For an intervention on the cause

$$\begin{aligned} \tilde{\Lambda}_X &\sim \mathcal{W}(n_0, \frac{I_K}{K}) \\ \tilde{\eta}_X | \tilde{\Lambda}_X &\sim \mathcal{N}(0, \frac{\tilde{\Lambda}_X}{n_0}). \end{aligned}$$

For an intervention on the effect

$$\begin{aligned} \tilde{B} = 0\tilde{\Lambda}_{Y|X} = \tilde{\Lambda}_Y &\sim \mathcal{W}(n_0, \frac{I_K}{K}) \\ \tilde{b} = \tilde{\eta}_Y | \tilde{\Lambda}_Y &\sim \mathcal{N}(0, \frac{\tilde{\Lambda}_Y}{n_0}). \end{aligned}$$